12

VSC-TR-82-12

MAGNITUDE: YIELD FOR NUCLEAR EXPLOSIONS IN GRANITE AT THE NEVADA TEST SITE AND ALGERIA: JOINT DETERMINATION WITH STATION EFFECTS AND WITH DATA CONTAINING CLIPPED AND LOW-AMPLITUDE SIGNALS

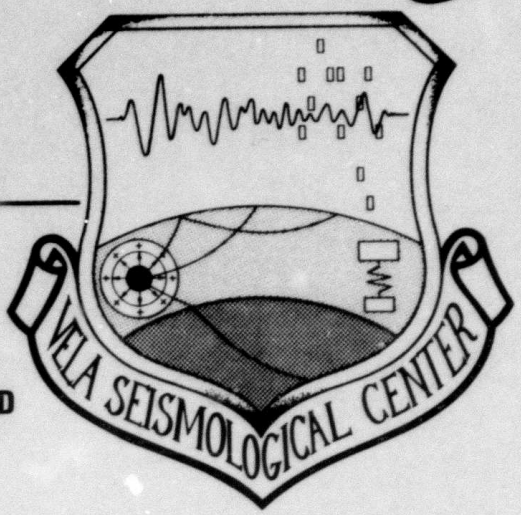

R. R. Blandford and R. H. Shumway

Seismic Data Analysis Center
Teledyne Geotech
314 Montgomery Street
Alexandria, Virginia 22314

23 FEB 82

APPROVED FOR PUBLIC RELEASE; DISTRIBUTION UNLIMITED.

Monitored By:
VELA Seismological Center
312 Montgomery Street
Alexandria, VA 22314

Unclassified

SECURITY CLASSIFICATION OF THIS PAGE (When Data Entered)

REPORT DOCUMENTATION PAGE		READ INSTRUCTIONS BEFORE COMPLETING FORM
1. REPORT NUMBER VSC-TR-82-12	2. GOVT ACCESSION NO. AD-A119137	3. RECIPIENT'S CATALOG NUMBER
4. TITLE (and Subtitle) MAGNITUDE:YIELD FOR NUCLEAR EXPLOSIONS IN GRANITE AT THE NEVADA TEST SITE AND ALGERIA: JOINT DETERMINATION WITH STATION EFFECTS AND WITH DATA CONTAINING CLIPPED AND LOW AMPLITUDE SIGNALS		5. TYPE OF REPORT & PERIOD COVERED 6. PERFORMING ORG. REPORT NUMBER SDAC-TR-81-16 ✓
7. AUTHOR(s) R. R. Blandford and R. H. Shumway		8. CONTRACT OR GRANT NUMBER(s) F08606-79-C-0007
9. PERFORMING ORGANIZATION NAME AND ADDRESS Teledyne Geotech 314 Montgomery Street Alexandria, Virginia 22314		10. PROGRAM ELEMENT, PROJECT, TASK AREA & WORK UNIT NUMBERS VT/0709/B/PMP
11. CONTROLLING OFFICE NAME AND ADDRESS VELA Seismological Center 312 Montgomery Street Alexandria, Virginia 22314		12. REPORT DATE 02/23/82 13. NUMBER OF PAGES 74
14. MONITORING AGENCY NAME & ADDRESS(if different from Controlling Office) Defense Advanced Research Projects Agency 1400 Wilson Boulevard Arlington, Virginia 22209		15. SECURITY CLASS. (of this report) Unclassified 15a. DECLASSIFICATION/DOWNGRADING SCHEDULE

16. DISTRIBUTION STATEMENT (of this Report)

APPROVED FOR PUBLIC RELEASE; DISTRIBUTION UNLIMITED.

17. DISTRIBUTION STATEMENT (of the abstract entered in Block 20, if different from Report)

18. SUPPLEMENTARY NOTES

19. KEY WORDS (Continue on reverse side if necessary and identify by block number)

Magnitude, Yield, Granite — Nevada Test Site — Clipping
PILEDRIVER, SAPHIRE, SAPHIR — Censored Data — Absorption
General Linear Model — Maximum Likelihood
Joint Maximum Likelihood — Expectation-Maximization — Distance-Amplitude

20. ABSTRACT (Continue on reverse side if necessary and identify by block number)

A systematic approach to short-period magnitude estimation has been developed and applied. The approach uses newly developed statistical techniques in the general linear model (GLM) which allow for the problems of clipping and of signals hidden by noise. Measurement procedures are outlined and the overall approach is first applied to four events in granite; PILEDRIVER, SHOAL, SAPHIRE, and RUBIS. The WWSSN short-period network film recordings, with the application of this approach, form an ideal network for shots over 10 kt in hard rock.

DD FORM 1 JAN 73 1473 EDITION OF 1 NOV 65 IS OBSOLETE

Unclassified

SECURITY CLASSIFICATION OF THIS PAGE (When Data Entered)

After correction for the effects of pP, estimated via synthetic waveform calculations, the magnitudes follow a theoretical magnitude:yield curve which changes from a slope of 1.0 near 10 kt to a slope of 0.8 near 100 kt.

The offset between the US and Sahara explosions is 0.04 to 0.12 m_b units, with US events biased low. It is not clear from the data if this is due to t^*, or to coupling differences.

Station corrections determined from a suite of 9 explosions at different test sites around the world show good correlation with residuals estimated by North (1977).

MAGNITUDE:YIELD FOR NUCLEAR EXPLOSIONS IN GRANITE AT THE NEVADA TEST SITE AND ALGERIA: JOINT DETERMINATION WITH STATION EFFECTS AND WITH DATA CONTAINING CLIPPED AND LOW-AMPLITUDE SIGNALS

SEISMIC DATA ANALYSIS CENTER REPORT NO.: SDAC-TR-81-16

AFTAC Project Authorization No.:	VELA T/0709/B/PMP
Project Title:	Seismic Data Analysis Center
ARPA Order No.:	2551
Name of Contractor:	TELEDYNE GEOTECH
Contract No.:	F08606-79-C-0007
Date of Contract:	27 October 1978
Amount of Contract:	$2,191,475
Contract Expiration Date:	30 September 1983
Project Manager:	Robert R. Blandford (703) 836-3882

P. O. Box 334, Alexandria, Virginia 22313

APPROVED FOR PUBLIC RELEASE; DISTRIBUTION UNLIMITED.

ABSTRACT

A systematic approach to short-period magnitude estimation has been developed and applied. The approach uses newly developed statistical techniques in the general linear model (GLM) which allow for the problems of clipping and of signals hidden by noise. Measurement procedures are outlined and the overall approach is first applied to four events in granite; PILEDRIVER, SHOAL, SAPHIRE, and RUBIS. The WWSSN short-period network film recordings, with the application of this approach, form an ideal network for shots over 10 kt in hard rock. After correction for the effects of pP, estimated via synthetic waveform calculations, the magnitudes follow a theoretical magnitude:yield curve which changes from a slope of 1.0 near 10 kt to a slope of 0.8 near 100 kt.

The offset between the US and Sahara explosions is 0.04 to 0.12 m_b units, with US events biased low. It is not clear from the data if this is due to t*, or to coupling differences.

Station corrections determined from a suite of 9 explosions at different test sites around the world show good correlation with residuals estimated by North (1977).

TABLE OF CONTENTS

LIST OF FIGURES

LIST OF FIGURES (CONTINUED)

LIST OF FIGURES (CONTINUED)

LIST OF TABLES

LIST OF TABLES (CONTINUED)

INTRODUCTION

Several authors have approached the subject of determining yield from m_b in a systematic way; e.g. Evernden (1967), Ericsson (1971a,b), Springer and Hannon (1973), von Seggern (1977), Dahlman and Israelson (1977), and most recently Marshall, Springer, and Rodean (1979).

Others have concentrated on the techniques of determining network magnitudes from the individual station magnitudes; among these the work of von Seggern (1973), Christofferson et al. (1975), Ringdal (1976), and von Seggern and Rivers (1978) have been prominent.

In determining magnitudes, it is most important to have an accurate distance-amplitude relationship. The earliest such relationship was from Gutenberg and Richter (1956); in this study we use the relationship of Veith and Clawson (1972), which represents an average of explosion data over several test sites. When, on occasion, we choose to use data at distances larger than 95 degrees, we use the relationships of Sweetser and Blandford (1973) for PKP phases.

The subject of station effects at short-period stations has received attention from many authors; the most systematic collection of station effects is perhaps that of North (1977), which was obtained by analysis of the readings reported to the ISC.

Only a few studies have addressed the subject of how to correct observed explosion magnitudes for the effects of pP. Blandford et al. (1976) showed from analysis of experimental data that the effect of pP could be large ($\lesssim .3$ m_b units), as did von Seggern (1977). Marshall et al. (1979) developed a systematic method of applying corrections for pP and did apply these corrections to a large body of data.

In this latter study, Marshall et. al. also applied corrections for differing levels of absorption under source and receiver. While this study was probably the most careful and complete study of magnitude/yield ever written, it did suffer from a number of weaknesses. Foremost among these was the small number of observations for many of the events. This makes even more serious the fact that the study did not use the

techniques of Ringdal (1976) in order to minimize bias from non-detection of small signals. Of course it was impossible for Marshall et al. to do this because no mathematical apparatus existed which made it possible to simultaneously determine station corrections and take account of the biasing effects of noise.

The major advance of technique in the present study is to remove this restriction which hampered Marshall et al., by developing a generalization of the general linear model which can take account of noise and clipping levels. In addition, we actually model the waveforms of the events of interest, in order to determine the pP correction instead of simply using a standard waveform for all yields as did Marshall et al.

DATA MEASUREMENTS

In order to assure the greatest degree of commonality between stations and events in this study, we have exclusively used the WWSSN short period film data. While use of this data has been difficult in the past due to its susceptibility to either clipping or masking by system or earth noise, the advent of the ability to allow for noise and clipping within the context of the general linear model eliminates these difficulties and "transforms" the WWSSN network into the best possible network for all except small events. The WWSSN network becomes so valuable because data with a constant instrument response can be found over such a large range of time and with good distribution around all test sites. It is worth remarking, however, that, if possible, film analysis should be confined to pre-1978 events since, in that year, a new format of film reproduction began in which there is much less resolution.

The full WWSSN network was analyzed for each event. A blanket request was made for all available data, and in general terms for about 90% of the stations film chips were received. About 20% of the these chips were unusable because of poor film development, timing failure, missing Z component, etc.

Table I shows the film reading procedures that were given to the analysts to ensure that proper noise readings were made if the signal was not visible.

TABLE I

Film Reading Procedures Used in this Study

1. Read the a (zero-crossing to first peak), b (first peak to first trough), and max peak-to-trough or trough-to-peak in first 5 seconds in millimeters. Record readings in millimeters in the data file. Also, record gain as written on film and as seen with particular viewer.

2. Measure period for max as peak-to-peak or zero-crossing to zero-crossing or trough-to-trough as in your judgement best reflects the period of the maximum energy.

3. If a weak signal must be measured then try to find a strong signal from the same test site and by correlation try to establish if a particular cycle is a or b. In general, it is good practice to analyze events in pairs, with any weak events paired with a strong event.

4. If it is not possible to determine the exact location of the a or b cycles then the first clear down-swing is to be used to place a "noise" limit on the b cycle; that is, the true b amplitude is less than or equal to that down-swing. Similarly for the a phase if there is a clear up-swing which cannot confidently be said to be the a phase.

5. More commonly, however, there will be no clear up-swing; in this case a noise measurement must be made, and to do so search the preceding 20 seconds for the largest peak-to-trough excursion in the 1-2 Hz frequency range. (For the a phase find the largest zero-to-peak.) Often such amplitudes are less than 1 mm on WWSSN film. The period is to be recorded as 1 Hz.

6. Of course, if no arrival at all can be discerned then again a noise measurement must be made.

7. If the data for any phase are "wiped out" then an estimate of the clipping level must be made. To do this measure the amplitude of the largest "turning point" visible and multiply by 2. If you can be confident that the largest turning point is off the film then you could use the maximum distance to the edge of the film.

DATA ANALYSIS

In Table II we see the events studied in detail in this report, and in Figures 1a-d we see the magnitude versus distance plots for those events. The upward directed arrows indicate that the signal clipped and that the true magnitude is greater than that value; a downward directed arrow indicates a noise reading and that the magnitude is less than that value. We see that the data are consistent with the hypothesis that the amplitude distance curves are correct and that the magnitude is statistically constant as a function of distance.

Figure 2 is a plot of the amplitude-distance relationship for shallow earthquakes at typical depths of 40 kilometers and for distances greater than 90 degrees; in Table III the actual B factors used for 0 km depth are tabulated. These are to be used together with the Veith and Clawson curves for 0 depth. (Table III is for zero-to-peak measurements; it must be remembered that Veith and Clawson's tables are for peak-to-peak.)

The general linear model used on the measured noise and signal amplitude data is discussed in detail in Appendix I. Here we mention only that the method is an iterative one in which initial guesses as to the event magnitudes, station corrections, and magnitude standard deviations are updated in such a way that the likelihood of the new estimates is monotonically increasing. Also, it is worth mentioning that at each stage in the iteration, the amplitudes at those stations that do not observe the signal are estimated as being equal to the mean value so far computed, corrected by the station correction as so far computed, and adjusted by the most probable level of the true observation below noise or above the clipping level. These amplitudes are averaged at each stage in the iteration in order to give the magnitude estimate for the next stage in the iteration. The principal reference for this new procedure is that of Dempster (1977) and the extension to clipped and noise-hidden data was done by Aitkin (1981) and by Schmee and Hahn (1979).

TABLE II

Events Analyzed in this Study

EVENT	DATE	TIME	LOCATION	DEPTH (m)	YIELD (kt)
PILEDRIVER	66/06/02	15:30:00	37.07°N 116.07°W	462	62
SHOAL	63/10/26	17:00:00	39.20°N 118.30°E	367	12
RUBIS	63/10/20	13:00:00	24:02:07.8°N 05:02:19.0°E	---	52
SAPHIRE	65/02/27	11/30:00	24:03:31.4°N 05:01:52.3°E	645-785	120

Yields from Marshall et al (1979), depth of SAPHIRE from IAEA publication, November 1970. Locations of French shots from Bolt (1976).

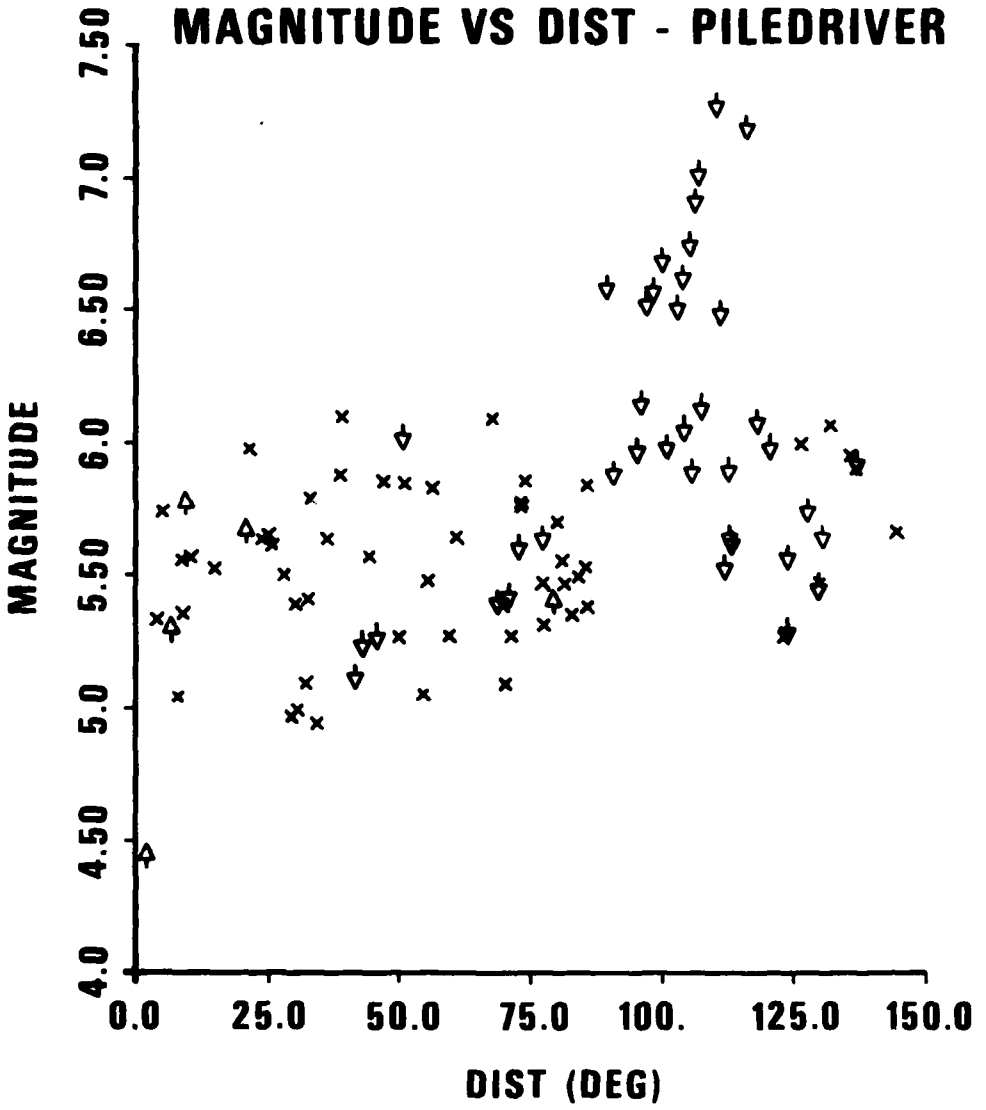

Figure 1a. Magnitude (max/GT) versus distance for PILEDRIVER. Downward and upward pointing arrows indicate noise and clipping limits respectively. The distance amplitude relation used is that of Veith and Clawson (1972) to 95° and of Sweetser and Blandford (1973) beyond, both for zero kilometers depth.

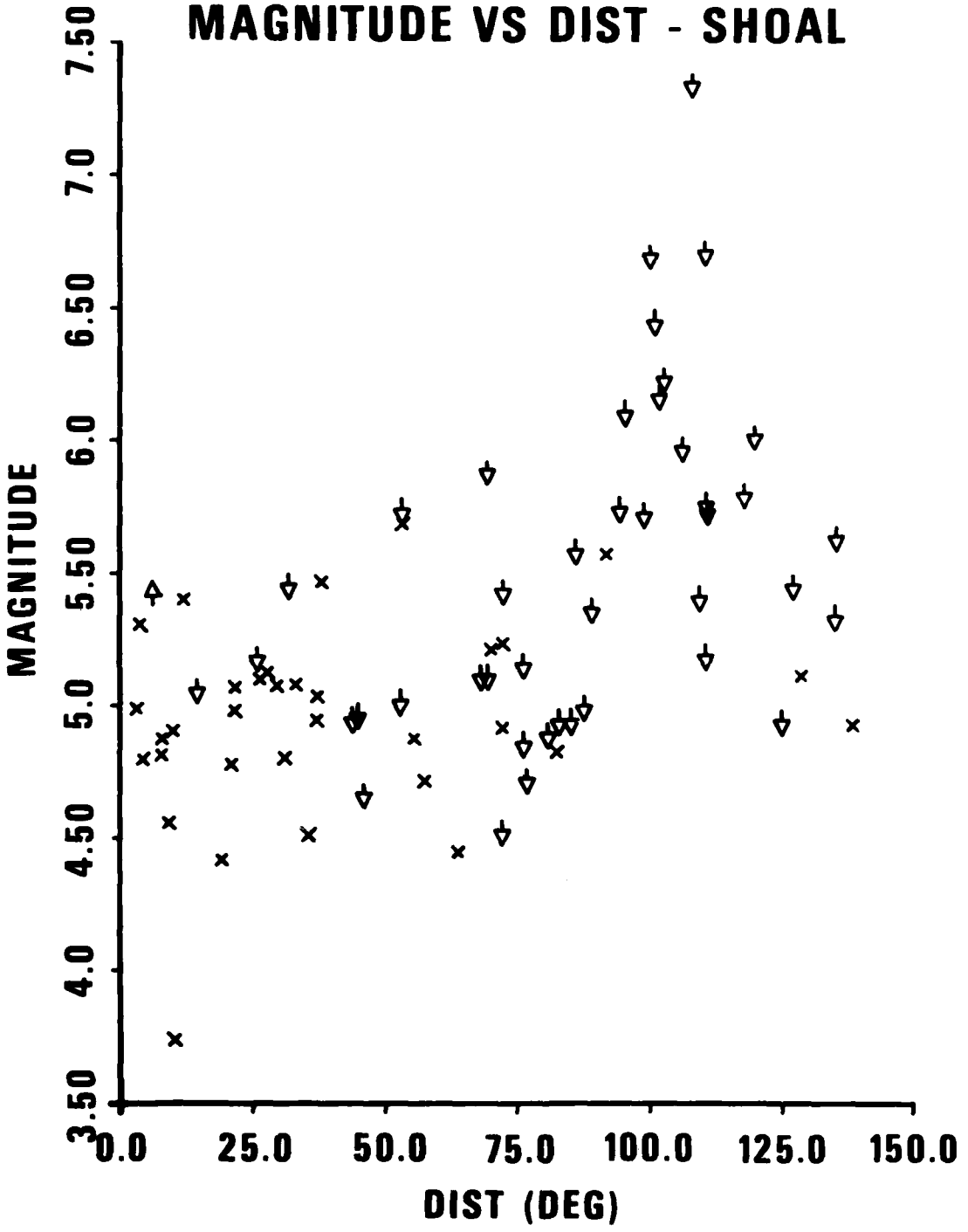

Figure 1b. Magnitude (max/GT) versus distance for SHOAL. Downward and upward pointing arrows indicate noise and clipping limits respectively. The distance amplitude relation used is that of Veith and Clawson (1972) to 95° and of Sweetser and Blandford (1973) beyond, both for zero kilometers depth.

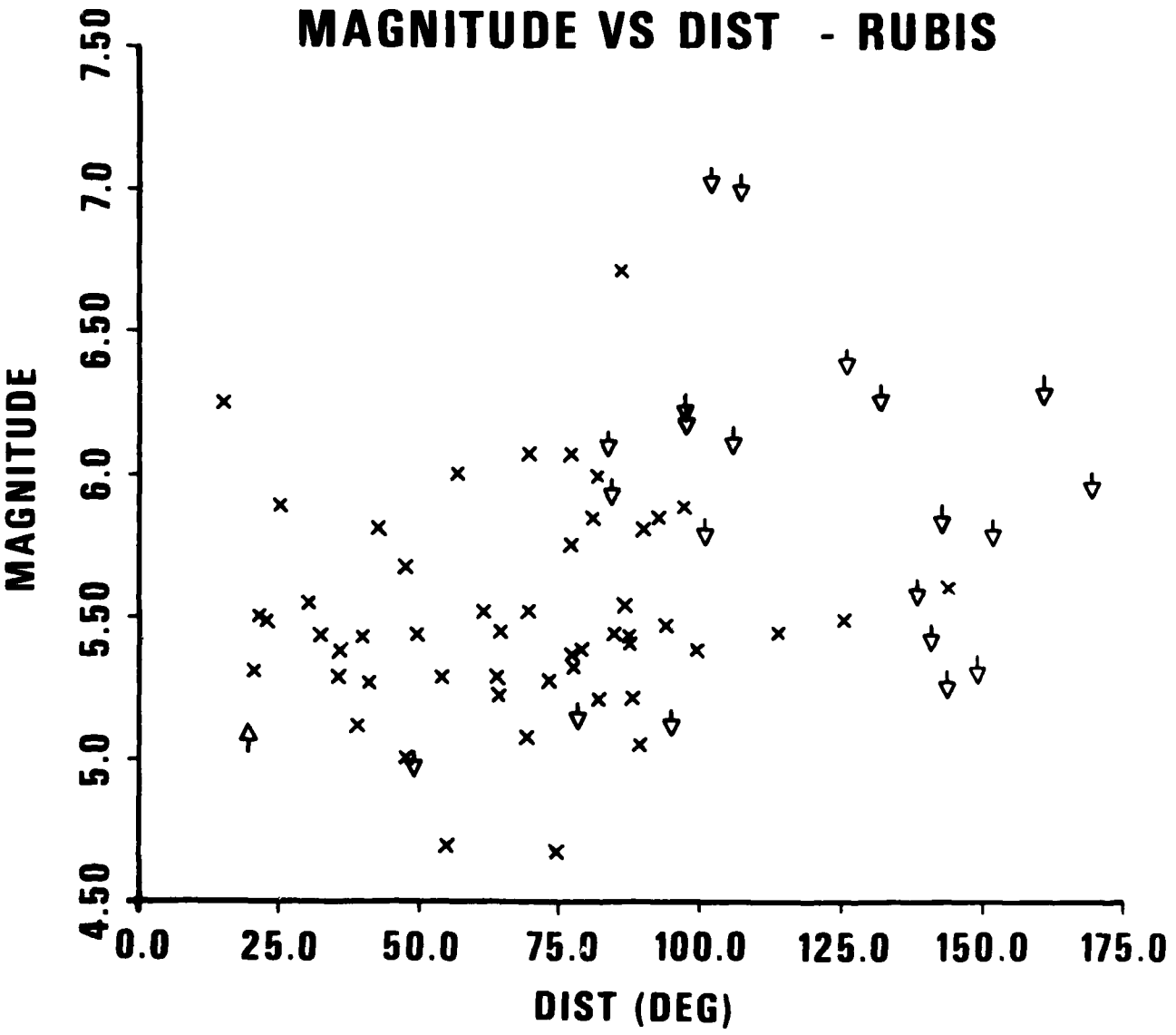

Figure 1c. Magnitude (max/GT) versus distance for RUBIS. Downward and upward pointing arrows indicate noise and clipping limits respectively. The distance amplitude relation used is that of Veith and Clawson (1972) to 95° and of Sweetser and Blandford (1973) beyond, both for zero kilometers depth.

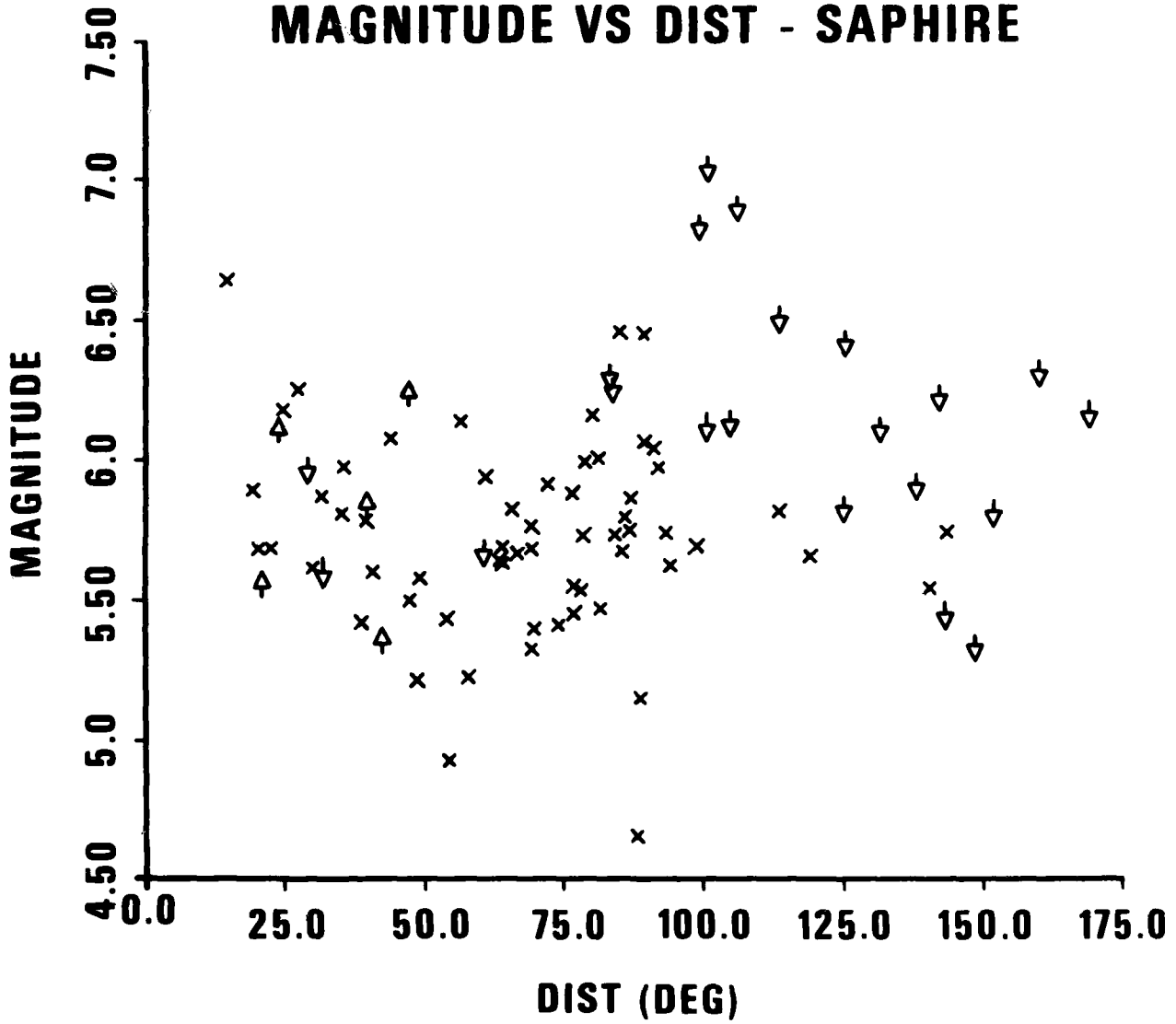

Figure 1d. Magnitude (max/GT) versus distance for SAPHIRE. Downward and upward pointing arrows indicate noise and clipping limits respectively. The distance amplitude relation used is that of Veith and Clawson (1972) to 95° and of Sweetser and Blandford (1973) beyond, both for zero kilometers depth.

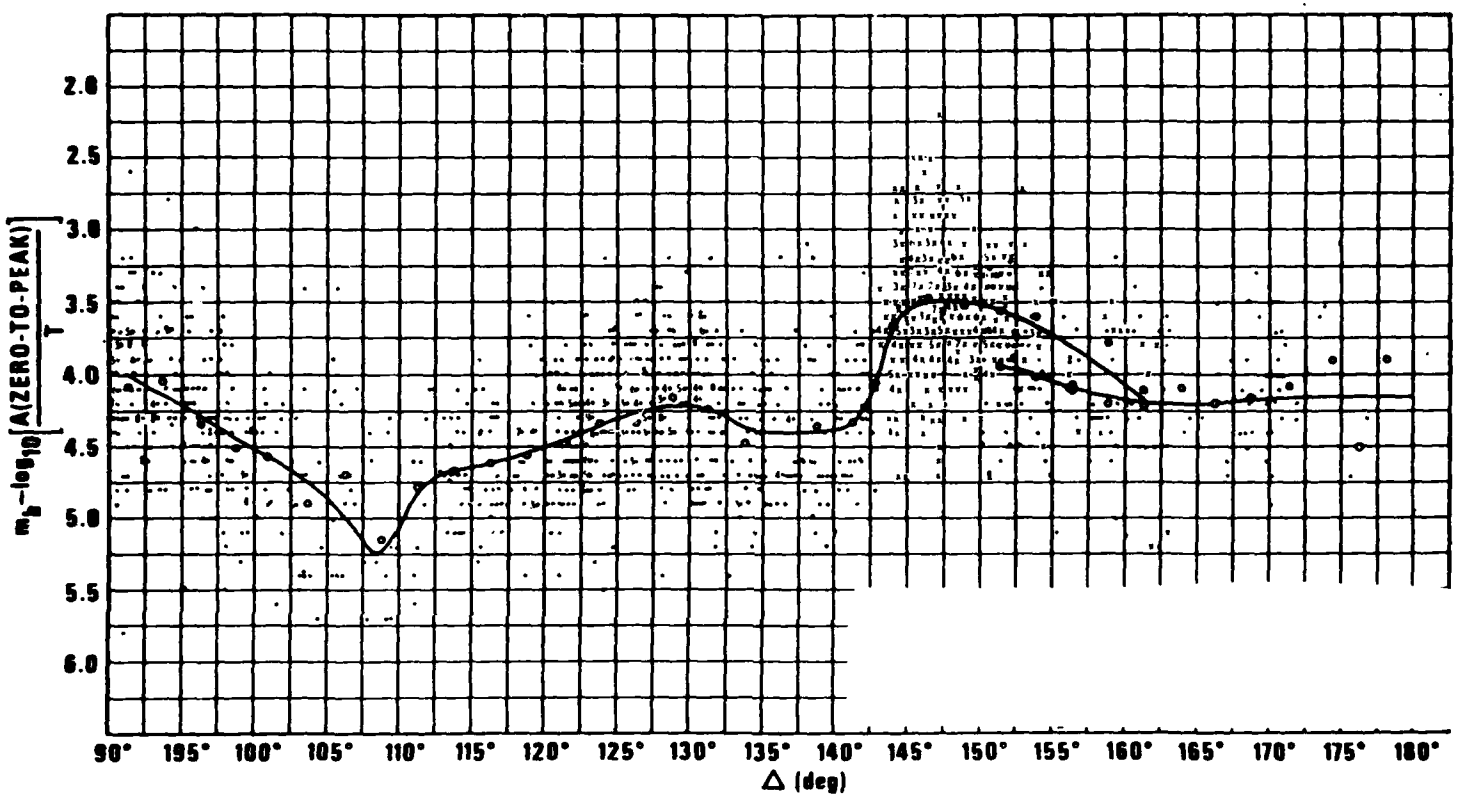

Figure 2. Amplitude-distance relation for first arrivals as reported by ISC bulletins for January-June 1970. Every event with depth less than 70 km and with two or more $\log_{10}$ (A/T) values reported for $\Delta > 110°$ were used. Occasional erroneous first picks which were truly PKP_2 were rejected on the basis of their time residuals. Average B factors were computed by subtracting the $\log_{10}$ (A/T) zero-to-peak value from the ISC m_b value, averaging the resulting values over 2.5° increments of distance, and drawing a smooth curve by hand through the results. Table III gives the numerical B values to be used for zero depth, which are obtained by adding 0.2. P, P_{diff}, and PKIKP are indicated by small dots. Initial arrivals which may be other phases are indicated by crosses. The larger points and circles are the 2.5° averages. The lower of the double branch from 152°-162° are late picks of PKP_2 from Sweetser and Blandford (1973).

TABLE III

B factors for zero-to-peak amplitudes corrected for instrument response at period T and divided by T in the distance range 95°-180°. To be used with maximum amplitude in the first 5 seconds of the first arrival for zero depth events (from Sweetser and Blandford (1973). To be used with Veith and Clawson (1972) for $\Delta < 95°$.

Distance (deg)	B	Distance (deg)	B
95	4.430	137	4.600
96	4.500	138	4.590
97	4.560	139	4.575
98	4.625	140	4.565
99	4.680	141	4.550
100	4.735	142	4.450
101	4.790	143	4.215
102	4.840	144	3.850
103	4.905	145	3.710
104	4.980	146	3.490
105	5.060	147	3.675
106	5.180	148	3.680
107	5.325	149	3.700
108	5.425	150	3.725
109	5.400	151	3.750
110	5.225	152	4.180
111	5.020	153	4.210
112	4.950	154	4.235
113	4.915	155	4.260
114	4.875	156	4.275
115	4.850	157	4.300
116	4.830	158	4.340
117	4.800	159	4.370
118	4.770	160	4.375
119	4.730	161	4.385
120	4.690	162	4.385
121	4.660	163	4.385
122	4.625	164	4.375
123	4.585	165	4.375
124	4.550	166	4.375
125	4.515	167	4.375
126	4.480	168	4.370
127	4.450	169	4.360
128	4.425	170	4.360
129	4.415	171	4.360
130	4.425	172	4.360
131	4.450	173	4.360
132	4.490	174	4.360
133	4.550	175	4.360
134	4.590	176	4.360
135	4.610	177	4.360
136	4.610	178	4.360

Application of this analysis procedure to the measurements for the four events in Table II yields the magnitudes in Table IV. Here we see that we have imposed the limitation that the distance be less than 95 degrees in order to conform to the standard definition of m_b magnitude. We also see that magnitudes have been calculated for the a, b, and max phase, using only the raw amplitudes, the amplitudes corrected for instrument response at the measured period, and corrected for instrument response and divided by period. For the max phase, this last measurement is in accord with the standard definition of m_b and it is this magnitude only which we shall discuss in the rest of this report, although for all events, the measurements have been made to enable calculation of the other magnitudes. The relationship between the magnitudes remains a subject for further research.

We may remark, however, on a few points of interest which can be seen on inspection of Table IV.

- Moving from the a to b phase, there is an increase of about 0.6 m_b units; from the b to max phase, there is a difference of about 0.25 m_b units, for a total difference from a to max of about 0.85 units.

- For all events except SHOAL, the magnitude increases slightly when corrected for instrument response, and then decreases when divided by period. For SHOAL it is the reverse, which may have to do with the dominant period of this smaller event. For SHOAL the magnitude, when corrected for instrument response and divided by period, is nearly identical to the case of magnitudes computed from raw amplitudes.

TABLE IV

m_b's calculated using the a, b, and max phase for 4 events for $\Delta < 95°$. Only amplitudes ≥ 2 millimeters on the viewing screen were used as signals; lesser amplitudes were used as noise estimates, i.e., the signal was judged to be smaller. This is believed to be the more valid procedure due to the difficulty of measuring such small amplitudes, and a tendency toward over-estimation. If all signal amplitudes are used, calculations show that the magnitudes are 0.02 m_b larger on the average.

	a	A/G	a/G	b	b/G	b/G	mx	mx/G	mx/GT
PILEDRIVER	4.649	+4.680	4.679	5.202	+5.227	5.227	5.473	+5.502	5.498
SHOAL	4.062	3.993	4.063	4.436	4.377	4.437	4.740	4.702	4.747
RUBIS	4.596	+4.675	4.648	5.178	+5.281	5.244	5.439	+5.553	5.508
SAPHIRE	4.879	+5.052	4.986	5.416	+5.591	5.522	5.688	+5.863	5.793

CORRECTION FOR t* AND FOR pP AND OTHER SOURCE EFFECTS

Before the m_b values reported in Table IV can be accurately related to yield, it is necessary to make corrections for the effects of pP and of absorption, much as was done by Marshall et al. (1979). To perform calculations of synthetic waveforms to evaluate the effects of pP, it is necessary to have the delay times. The delay times for RUBIS and SAPHIRE (τ=0.21, 0.27 sec) can be obtained from a 1970 IAEA publication, which also gives the velocity of the French granite as 5.25 km/sec (P. Marshall, personal communication). Marshall et al. (1979) also give the delay times for PILEDRIVER and SHOAL as (0.24, 0.21 seconds); however, Shumway and Blandford (1977) found the delay for PILEDRIVER to be 0.17 seconds; and cube root depth scaling would give the delay for SHOAL to be 0.15 seconds. Both sets of delays will be used in this study, and we shall see that there are significant effects resulting from such seemingly minor differences in pP delays.

Typical results of such calculations may be seen in Figure 3; the pP corrections may be obtained by subtracting the magnitude in the first column from the appropriate magnitude seen in the second or third column. The results of such calculations are seen in Table V. We have chosen to correct all of the events for pP and then to add a constant so that the PILEDRIVER m_b remains unchanged.

For example, the PILEDRIVER magnitude for the c phase corrected for instrument response and divided by T with the pP phase included is, from Figure 3, 3.65 (to within an arbitrary constant). Without pP the magnitude is 3.42. The difference is a decrease of 0.23 magnitude units. Now SAPHIRE decreases from 3.84 to 3.64, a decrease of only 0.19 units so that the 0.23 correction applied to SAPHIRE results in an increase from 5.79 in the fourth column of figures to 5.83 in the fifth. Notice also the significant differences between columns 5 and 6, for example changes of .08 m_b for RUBIS and SAPHIRE. This shows that apparently minor differences in pP delay times can have significant effects on m_b.

In Figure 4 we see plotted some of the m_b values from Table V. We

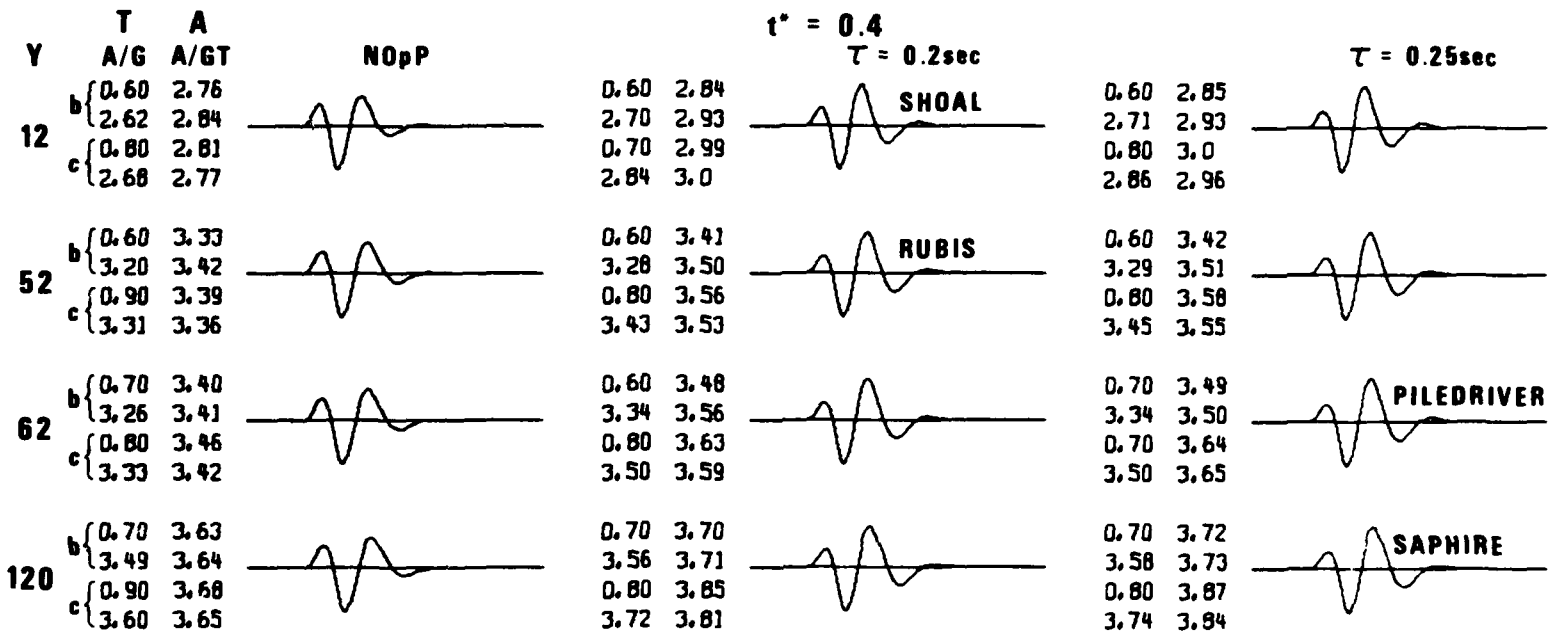

Figure 3. WWSSN synthetic signals composed of a direct and pP pulse from the von Seggern-Blandford granite model for the indicated yields, Y, delays and t* = 0.4. For the first column the pP reflection coefficient is zero, i.e. there is no pP. For the next two columns the reflection coefficient is $-0.5\,(1 + \exp(-f^2))$ where f is frequency. The parameters T (period), A(log amplitude), A/G(log(amplitude/G)) where G is the system response at T, and A/GT(log(amplitude/GT)) are measured by computer for the b and c phases.

TABLE V

Magnitude summary. The column headed by "WW" is taken from the last column of Table IV. The next column has the pP effect removed but corrected so that the PILEDRIVER m_b does not change. The next column is similar except that the pP time is taken to be 0.17 second instead of 0.24 for PILEDRIVER [see Shumway and Blandford (1977)], and SHOAL was taken as 0.15. (A special synthetic waveform calculation was performed for = 0.15.) We note a spread of as much as 0.08 m_b units between these last two columns. The final column gives a simple average of signals neither below the noise nor clipped on the WWSSN.

	Y	log Y		WW	pP .24	pP .17	WW Simple
PILEDRIVER	62	1.79	5.47	5.50	5.50	5.50	5.50
SHOAL	12	1.08	4.75	4.75	4.75	4.72	4.94
RUBIS	52	1.72	5.52	5.51	5.57	5.49	5.52
SAPHIRE	120	2.08	5.74	5.79	5.83	5.75	5.73

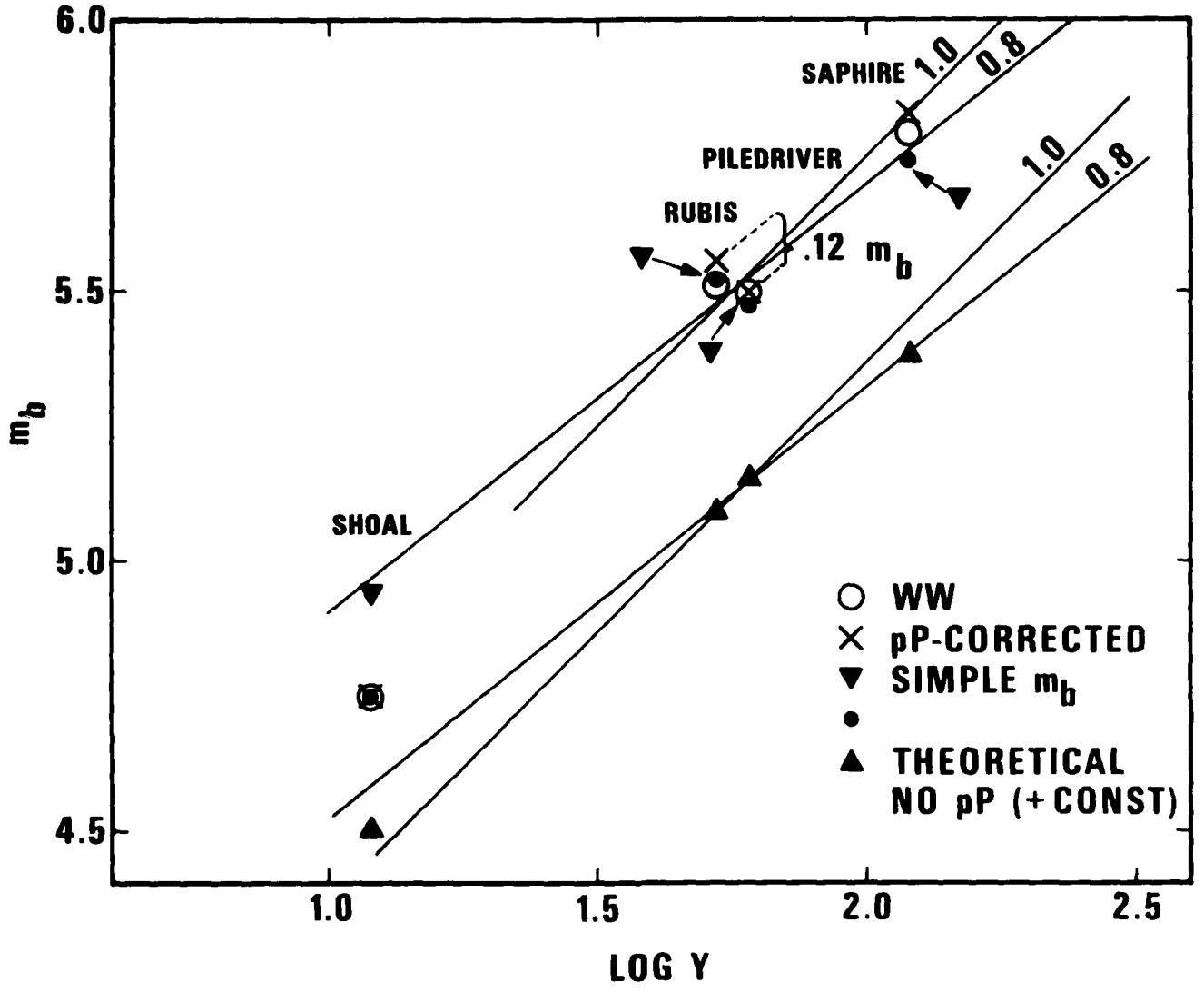

Figure 4. Experimental and theoretical m_b as a function of yield for the explosions PILEDRIVER, SHOAL, RUBIS, and SAPHIRE. The Worldwide m_b's calculated in this paper show an overall slope close to 1.0. When the changes due to pP are backed out (see Figure 3 and Tables IV, V assuming the delay for PILEDRIVER is 0.24 sec) then the slope becomes even closer to 1.0. The offset between PILEDRIVER and RUBIS implies that the effects of source coupling and relative attenuation between the two test sites result in a bias of 0.12 m_b with the Sahara having the higher magnitude for a fixed yield. If this offset is subtracted from the Sahara event corrected for pP then the resulting amplitude-yield curve changes from a low-yield slope of 1.0 to a high-yield slope of 0.8, in agreement with the theoretical variable slope, as can be seen in Figure 6.

see that the simple m_b values (m_b values which are the simple average of the detecting station magnitudes) have a slope of close to 0.8 as a function of yield. This effect is mostly due to the overestimate of the SHOAL magnitude. When the estimates which take account of noise and clipping levels are included, however, the slope becomes close to 1.0; and when the further corrections are made for pP, assuming the pP delay for PILEDRIVER is 0.24 seconds, then the slight increase in m_b for SAPHIRE leads to an even closer fit to a 1.0 slope.

The dashed lines touching the RUBIS and PILEDRIVER events indicate an offset of 0.12 m_b units between the NTS and Sahara test sites. (Use of a pP delay for PILEDRIVER of 0.17 seconds would yield an offset of only 0.04 m_b.) We may ask if this offset could be due to absorption.

In Figure 5 we see the ratios of PILEDRIVER spectra divided by spectra due to either SAPHIRE or RUBIS. Considering the spectra as a whole, one could not reject the hypothesis that the trend with frequency was due to a relative t* between the test sites of t* = 0.06; a value which would explain an offset of 0.08 m_b units. However, it is notable that between about 1 and 2.5 Hz there is quite a steep slope corresponding to a relative t* of about 0.4. If this truly represented the difference in t* between NTS and the Sahara, then one would expect the NTS m_b to be as much as 0.6 m_b lower than the Sahara m_b instead of the observed 0.12 m_b. Thus one is immediately tempted to assert that the apparent large slope between 1 and 2.5 Hz is simply an artifact.

On the other hand, Dahlman and Israelson (1977) write that the cavity size from the French tests was substantially smaller than that expected on the basis of NTS tests. If so, then the French tests may be small because of some unknown coupling factor; and the NTS explosions coincidentally small because of high absorption. The data basically are insufficient to resolve such complicated questions.

As a marginal remark, one may speculate that if there were indeed substantially larger attenuation under NTS than under the Sahara, then the turnover of the spectral ratio near 1 Hz in Figure 5 may be due to the poor reflection of pP in the Sahara due to the fact that the

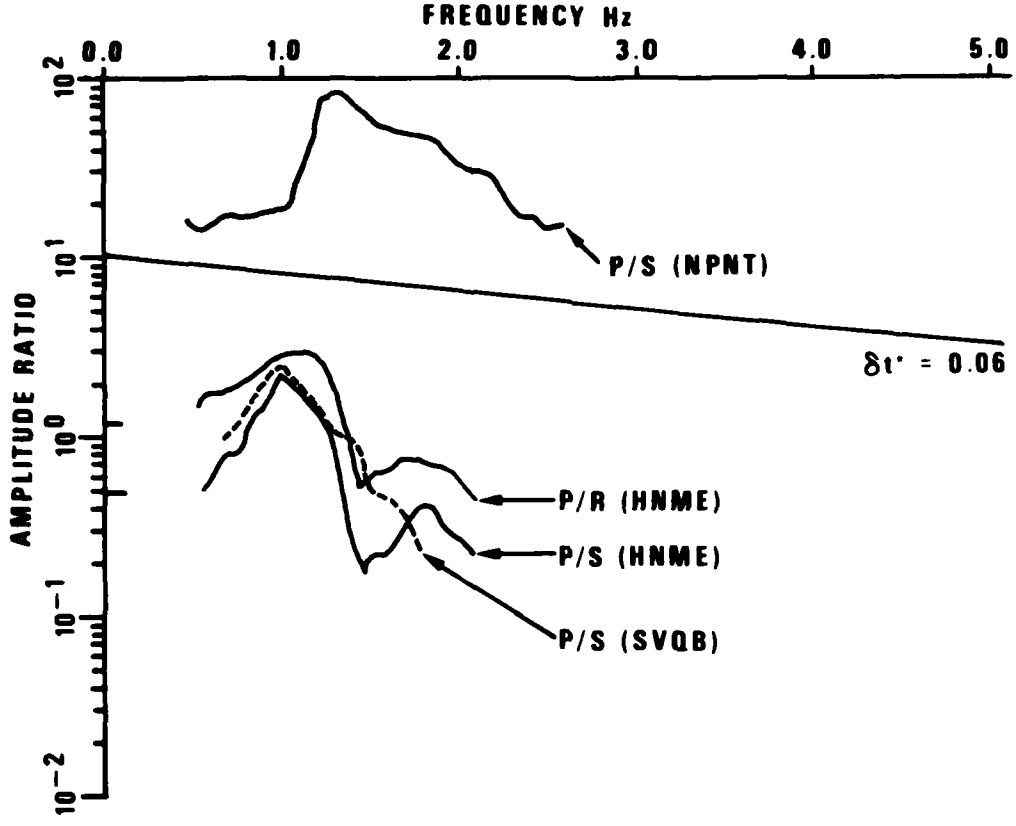

Figure 5. Spectral ratio of the first 6.4 seconds of P waves for PILEDRIVER/SAPHIRE and for PILEDRIVER/RUBIS. Note that at NPNT the ratio is about 30, whereas in theory it should be nearly constant at about 0.5. This is perhaps due to defocussing. It is probably not due to differential Q, otherwise there would be a greater slope to the ratio. For the other ratios, the trend below 1 Hz is toward the proper low-frequency limit of the yield ratios as indicated by tick marks on the vertical axis. The change in slope around 1 Hz may reflect higher t* at NTS and poorer pP reflection at Hoggar below 1 Hz due to the extreme relief O(1:1) of the massif.

explosions were detonated in the Hoggar massif, which in profile is approximately 1 km high and 2 kilometers wide. If the reflection is poor, then the P-wave amplitude at low frequencies from the Hoggar would not be efficiently cancelled by pP and the NTS/Sahara ratio would decline toward low frequencies, as observed. If this were the case than one would deduce that poor coupling in the Sahara is being offset by high absoption under NTS.

Returning to Figure 4, we let the source of the 0.12 m_b offset remain undecided and simply shift the two Sahara shots down by 0.12 m_b. The result is seen in Figure 6 and we see that the observed m_b:yield curve is similar in shape to the theoretical curve. The only major discrepancy is that the SHOAL event m_b is too small. This may, perhaps, be within the margin of error for this small event at a site rather distant from NTS.

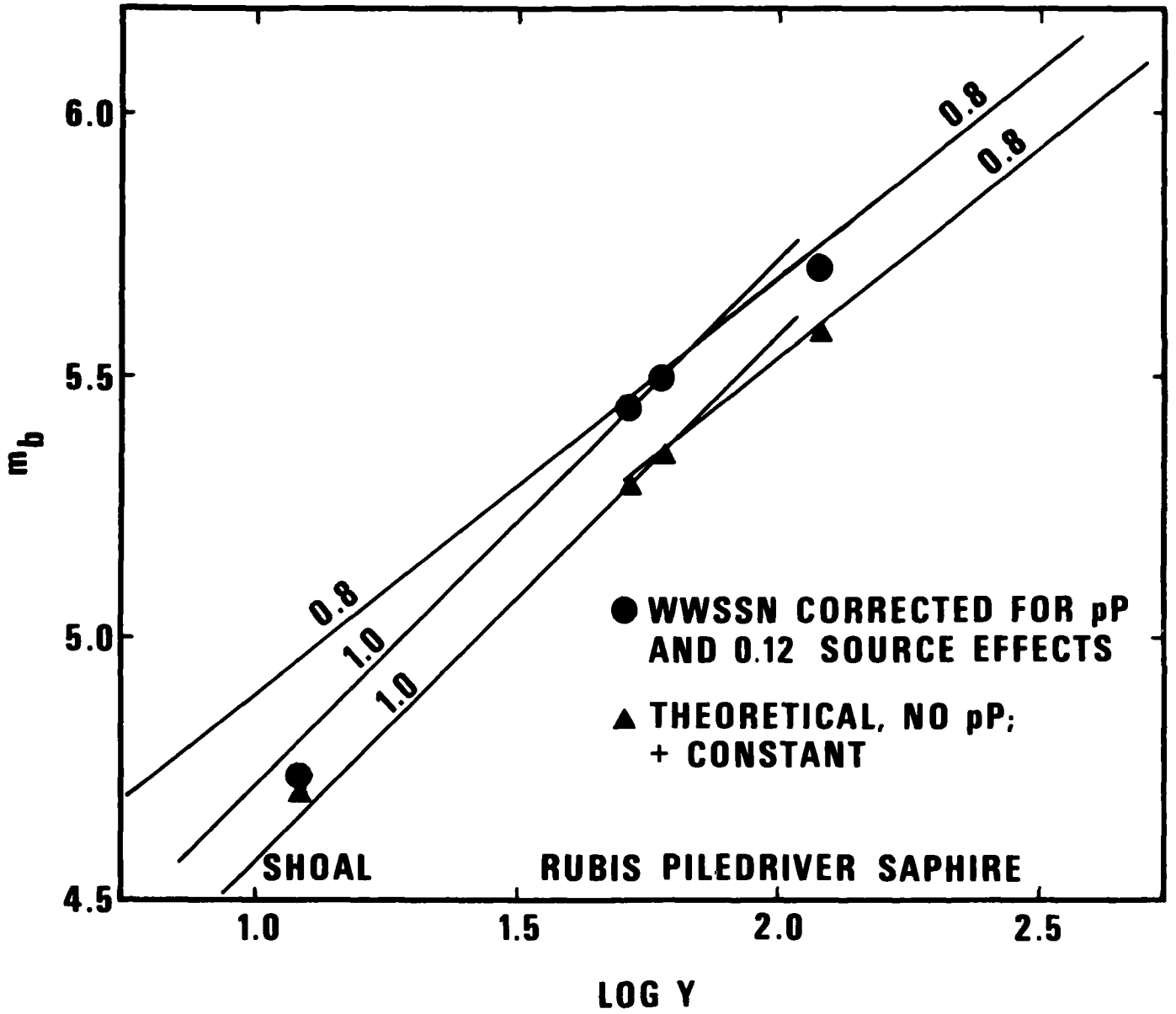

Figure 6. WWSSN m_b's corrected for pP and source bias give a variable slope ranging from 1.0 near SHOAL to 0.8 near SAPHIRE. For yields near 150 kt the correct slope is 0.8 after correction for pP. This correct answer could have been obtained in several other ways, e.g. the simple slope between RUBIS and SAPHIRE without correction for pP, and (incorrectly) as the simple slope from SHOAL to SAPHIRE of the WWSSN m_b's averaging only detected signals.

STATION EFFECTS

The station effects which were calculated in the course of producing the magnitudes in Table V and Figures 4 and 6 are the appropriate ones for a comparison of magnitudes between the NTS and Sahara test sites. If one wanted to add one more test site, e.g., Semipalatinsk, then there would be a different set of station corrections. However, we may be interested in an estimate of station corrections for which the peculiarities of the source-station paths have been averaged out, resulting in station corrections which fairly closely represent the near-receiver structure and absorption. For this purpose one would want to have as well-distributed a set of events as possible, without overly weighting any particular test site.

For this purpose, we have measured the entire WWSSN network for the events listed in Table VI. The first 9 of these events were then used to determine station corrections, and these station corrections were used to determine the magnitudes of the last five events in Table VI. Actually the Table VI magnitudes and corresponding station corrections were determined using only readings for distances less than 95 degrees. Thus these magnitudes are perhaps the most authoritative available in an absolute sense. We note that there are small changes, averaging a decrease of 0.02 m_b units as compared to the magnitudes in Table V. It is important to remember, however, that the magnitudes in Table V are the ones to use for comparison of the NTS and Sahara test sites.

To determine station corrections, however, it is useful to allow PKP readings; otherwise many stations do not have sufficient readings to define the station effects. Carrying this through for the first 9 events in Table VI, we plot the results versus the station corrections determined by North (1977), as seen in Figure 7. By no means all of the WWSSN stations can be found in North's list, and North determined station corrections for many non-WWSSN stations. In Figure 7 we see that, in general, there is a definite correlation; however, there are several stations for which the North corrections are too large. We interpret this to show that the poorer stations tend to detect only the anomalously large amplitudes. As a result, North's analysis, which

TABLE VI

Event magnitudes from entire WWSSN network using max/GT and $0 < \Delta < 95°$ with station corrections common to all events. The events PILEDRIVER, RUBIS, SAPHIRE, and SHOAL decrease in magnitude an average of 0.02 units as compared to Tables IV and V. In this calculation, the absolute magnitude for these events are more reliable, but the relative magnitudes less reliable since the station corrections are less finely tuned to the NTS and Sahara test sites. If magnitudes are determined for $0 < \Delta < 180°$ there is typically an increase by 0.05 m_b, except that the Tuomoto m_b, weak and strongly affected by PKP, increase by 0.14 m_b.

Event	Date	Latitude	Longitude	m_b
Piledriver	66/06/02	37.23°N	116.06°W	5.49
Rubis	63/10/20	24.00°N	5.00°E	5.45
Azgir	76/07/29	47.782°N	48.120°E	5.84
Novaya Zemlya	76/10/20	73.00°N	55.00°E	4.76
Kazakh	73/12/14	50.04°N	79.01°E	5.76
Tuomoto	77/02/19	22.10°N	138.76°W	4.66
China	76/10/17	41.00°N	89.00°E	4.56
Salmon	64/10/22	31.14°N	89.57°W	4.40
Longshot	65/10/29	51.44°N	179.18°E	5.90
Shoal	63/10/26	39.20°N	118.38°W	4.75
Saphire	65/02/27	24.06°N	5.03°E	5.72
Kazakh	69/09/11	49.70°N	78.11°E	4.57
Kazakh	78/09/15	49.91°N	78.94°E	5.76
Azgir	77/09/30	47.800°N	48.145°E	4.81

Station corrections determined with first 9 events in list.

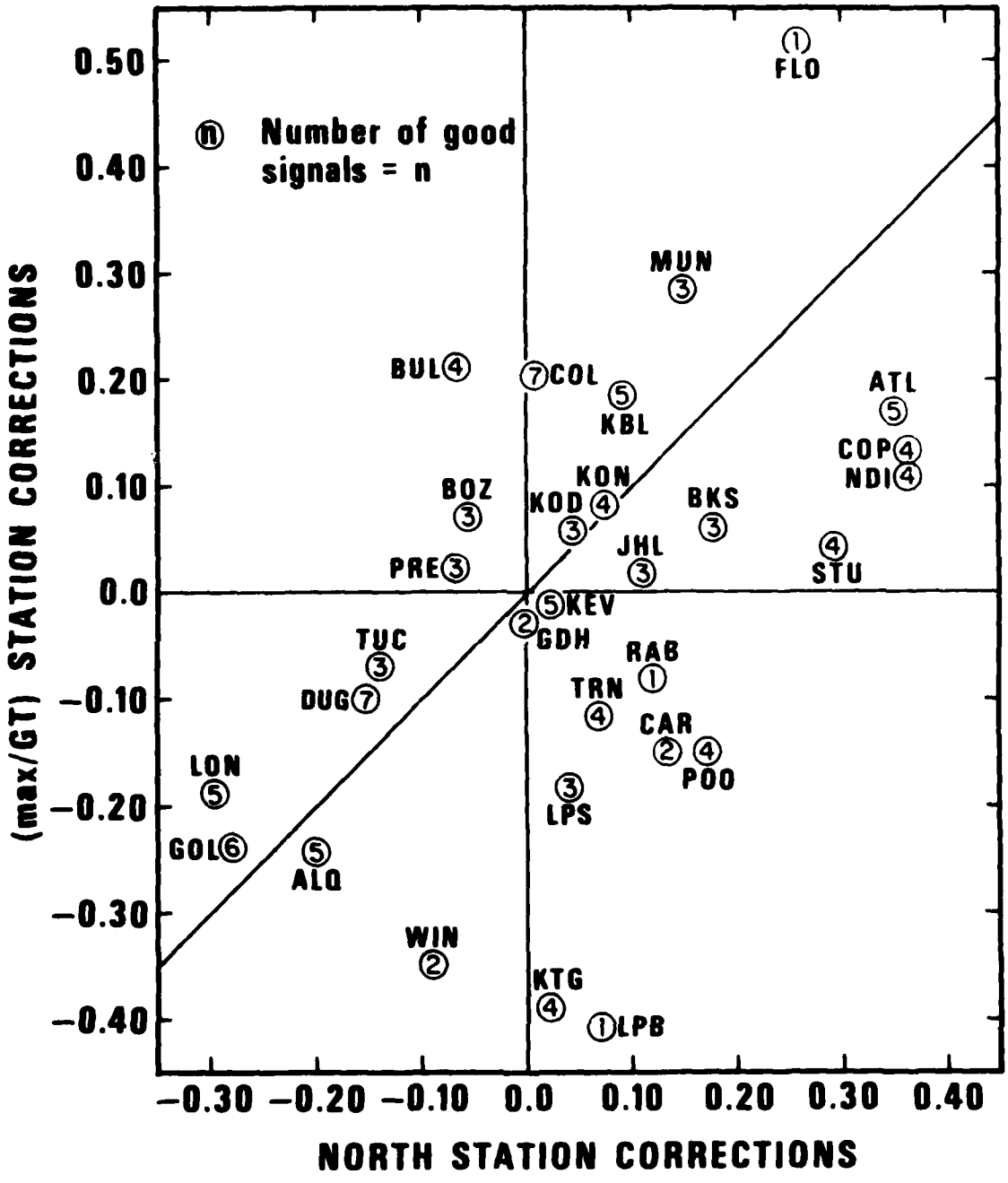

Figure 7. Station corrections for the events in Table VIII (but using data from the distance range $0° < \Delta < 180°$ for completeness) as a function of station corrections due to North (1977) which were derived from ISC earthquake dates.

could make no allowance for noise, would tend to overestimate the station correction. Some support for this may be garnered from the fact that stations which are generally regarded as sensitive and well-run, such as ALQ, GOL, COL, KBL, BKS, and KON do tend to lie close to the line through the origin with slope 1.0.

Improvement of these station corrections could be achieved by such approaches as adding data from Gasbuggy, Rulison, Faultless, a bigger event from Tuamoto, Soviet PNE's, and shots from Novaya Zemlya. It would be useful also to add more events from the established test sites in order to fill in stations which did not observe the selected event and to average out fluctuations which come even from within a test site. However, an extension of the present program is needed before this last calculation can be performed; for each event from a particular test site weights roughly inversely proportional to the number of events from that test site must be assigned in order to prevent overweighting of station corrections by a particular test site. This apparently simple modification calls for rather substantial changes in the computation techniques.

In a preliminary attempt to see at what distance between events the station corrections became independent of each other, station corrections were computed for pairs of events at increasing distances from each other. As the distance between events increased, it was expected that the residual variance would increase. We found that this was the case, and also that it was necessary, in order to obtain an unbiased estimate of the standard deviation, to divide the total variance not by the number of stations x events, but by the number of observations, including noise and clipping observations.

When this was done, we found that for the two event pairs with separations of approximately 3 kilometers (RUBIS-SAPHIR and AZGIR 07/76-09/77), the standard deviation was about 0.12 m_b; but that for event pair separations from 15 kilometers out to 100 degrees, the computed residual standard deviations were not statistically different from 0.3 m_b.

As a final task in this study we surveyed the geological literature to find crustal models for each of the WWSSN stations. The details of these crustal models may be found in Appendix II. Using these crustal models, a synthetic waveform was computed using a causal wavelet from a 50 kt explosion through a t* of 0.4 and a WWSSN SP response. The peak to trough maximum amplitude of the waveforms were measured, the logarithms were taken and the mean removed. The results are displayed in Table VII. Application of these corrections should reduce the variance of the magnitude residuals, but will not change the mean value if observations are made at all stations. Future research should test whether or not these corrections do in fact reduce the observed variance.

TABLE VII

Station crustal corrections for WWSSN stations based on the crustal models given in Appendix II. The corrections are the log of the maximum peak amplitude of a 50 kt explosion in granite with a von Seggern-Blandford source spectrum, and a t* of 0.4 as seen through the WWSSN short-period response. The mean of the logs has been subtracted out before tabulation so that the net effect on a worldwide network would be zero. The observed magnitude should be equal to the expected magnitude plus the correction.

AAE	-0.061	DAV	-0.048	LPB	0.071	RCD	0.160
AAM	0.069	DUG	-0.059	LPS	-0.059	RIV	0.019
ADE	-0.059	ESK	0.001	LUB	0.079	RKO	-0.059
AFI	-0.059	FLO	-0.040	MAL	-0.020	SBA	-0.059
AKU	-0.059	GDH	-0.059	MAN	-0.059	SCP	-0.059
ALQ	-0.059	GEO	-0.059	MAT	-0.048	SDB	-0.059
ANP	-0.047	GIE	-0.048	MDS	-0.059	SEO	-0.059
ANT	-0.020	GOL	-0.059	MNN	-0.022	SHA	0.247
AQU	-0.036	GSC	-0.059	MSH	-0.059	SHI	0.060
ARE	-0.040	GUA	-0.037	MUN	-0.059	SHK	-0.059
ATL	-0.059	HKC	-0.059	NAI	-0.059	SHL	0.001
ATU	0.001	HLW	0.056	NAT	0.079	SJG	-0.048
BAG	-0.023	HNM	-0.036	NDI	0.059	SNA	0.252
BEC	0.142	HNR	0.050	NNA	-0.059	SNG	-0.059
BHP	0.140	HOW	0.124	NOR	0.050	SOM	0.079
BKS	-0.008	IST	-0.059	NUR	-0.059	SPA	0.100
BLA	-0.148	JCT	0.056	OGD	-0.058	STU	0.001
BOG	0.041	JER	0.079	OXF	0.079	TAB	-0.048
BOZ	0.054	KEV	-0.059	PDA	0.026	TAU	0.116
BUL	-0.067	KIP	-0.059	PEL	0.050	TOL	0.208
CAR	0.050	KOD	0.124	PMG	0.249	TRI	0.079
CHG	-0.059	KON	-0.059	POO	-0.059	TRN	-0.059
CMC	-0.059	KTG	-0.059	PRE	-0.059	TUC	0.046
COL	-0.059	LAH	0.259	PTO	-0.059	UME	-0.059
COP	-0.016	LEM	-0.048	QUE	0.050	VAL	-0.059
COR	0.075	LON	-0.059	QUI	-0.065	WEL	0.056
CTA	-0.059	LOR	0.050	RAB	-0.059	WES	-0.059
DAL	-0.018	LPA	0.124	RAR	-0.048	WIN	-0.059

SUMMARY AND SUGGESTIONS FOR FURTHER RESEARCH

By use of newly developed mathematical analysis techniques, the full WWSSN short-period network has been used to obtain unbiased magnitude estimates for four shots in granite; PILEDRIVER, SHOAL, SAPHIRE, and RUBIS. After correction for pP, there appears to be an offset between the US and Sahara shots of 0.04 to 0.12 magnitude units. If this offset is eliminated, then the magnitude/yield curve agrees with a theoretical curve in that the slope changes from 1.0 from 10 to 50 kt, to 0.8 from 50 to 100 kt. The data are inadequate to determine if this offset is a result of mantle absorption, poor pP reflection at low frequencies, or differences in coupling between US and Sahara granite.

Magnitudes have also been estimated for 10 additional events including events from Azgir, Novaya Zemlya, East Kazakh, Tuomoto, China, Mississippi (Salmon) and Amchitka (Longshot). The station corrections have been determined simultaneously for all these source mechanisms so that the magnitudes of all of these source regions are connected to each other in a consistent manner.

The station corrections determined from this suite of 9 source regions have been plotted versus the corrections of North (1977) and show substantial correlation. The correlation is best for those stations thought to be the best run. This is in agreement with the idea that at the poorer stations only the abnormally large arrivals would be reported to the ISC, the source of the data used to determine North's corrections.

Further research should proceed along the lines of:

- o Determine pP delay times directly from the data instead of from a priori information.
- o Generalize the mathematical procedures so that several events can be used from a test site without biasing the station corrections.

- Apply *a priori* station corrections and see if the estimated variance decreases.

- Better delineate the distance at which the residual variance after station corrections increases from 0.12 to 0.3 m_b units.

- Further check the idea that the station corrections determined in this study are superior to those from earlier studies by using an objective measure of station quality such as reporting threshold and plotting this measure versus the difference between the corrections determined in this study and those determined in other studies.

- Measure additional events with known yields such as Gasbuggy, Faultless, and Rulison; and improve the estimation of station effects by measuring shots in other test sites.

- Extend the analysis to M_s magnitude.

REFERENCES

Aitkin, M. (1981). A note on the regression analysis of censored data. Technometrics 23 161-163.

Baker, R. G. (1970). Determining magnitude from Lg, Bull. Seism. Soc. Am., 60, p. 1907-1919.

Basham, P. W., 1969, Canadian magnitudes of earthquakes aand nuclear explosions in south-western North America, Geophys. J. R. Astr. Soc., 17, p. 1-13.

Basham, P. W., and R. B. Horner, 1973, Seismic magnitudes of underground nuclear explosions, Bull. Seism. Soc. Am., 63, p. 105-132.

Berg, J. et al, 1966, Crustal refraction profile, Oregon Coast Range, Bull. Seism. Soc. Am., 56, p. 1357-1362.

Blandford, R. R. (1976). Experimental determination of scaling laws for contained and cratering explosions, SDAC-TR-76-3, Teledyne Geotech, P. O. Box 334, Alexandria, VA.

Blandford, R. R., M. F. Tillman, And D. P. Racine (1976). Empirical m_b:M_s relations at the Nevada Test Site with applications to m_b-yield relations, SDAC-TR-76-14, Teledyne Geotech, P.O. Box 334, Alexandria, VA.

Blandford, R. R., and P. K. Klouda, (1980), Magnitude-yield results at the Tonto Forest Observatory, in: "Studies of Seismic Wave Characteristics at Regional Distances", AL-80-1, Teledyne Geotech, Alexandria, Virginia.

Blandford, R., R. Hartenberger, and R. Naylor (1981). Regional amplitude-distance relations, discrimination, and detection. SDAC-TR-80-6, Seismic Data Analysis Center, Teledyne Geotech, P.O. Box 334, Alexandria, VA 22313.

Bollinger, G. A. (1973). Seismicity of the southeastern United States. Bull. Seism. Soc. Am., 63, p. 1785-1808.

Bolt, B. A., 1976, Nuclear Explosions and Earthquakes: The Parted Veil, W. H. Freeman and Co., San Francisco. 309 pp.

Booth, D. C., P. D. Marshall, and J. B. Young, (197). Long and short period P-wave amplitudes from earthquakes in the range 0-114°, Geophys. J. R. Astr. Soc., 39, p. 523-537.

Chang, A., and D. von Seggern, 1980, A study of amplitude anomaly and m_b bias at LASA subarrays, J. Geophys. Res., 85, p. 4811-4828..

Choubert, G. and Faure-Muret, A., 1980, Atlas Geologique du Monde, UNESCO, 1:10,000,000.

Christoffersson, L. A., R. T. Lacoss, and M. A. Chinney (1975). Estimation of network magnitude and station detection parameters. Semiannual Technical Summary, Seismic Discrimination 31 December 1975, Lincoln Laboratories, Lexington, Mass.

Cohen, A. C. (1959). Simplified estimators for the normal distribution when samples are singly censored or truncated, Technometrics, 1, p. 217-237.

Dahlman, O., and H. Israelson, 1977, Monitoring Underground Nuclear Explosions, Elsevier Scientific Publishing Company, New York. 440 pp.

Dempster, A. P., N. M. Laird, and D. B. Rubin, (1977). Maximum likelihood estimation from incomplete data via the EM algorithm. J. Roy. Statist. Soc. B., 39, 1-38.

Der, Z. A., D. W. Rivers, T. W. McElfresh, A. O'Donnell, P. J. Klouda, and M. Marshall, 1981, Q of the earth in the 0.5-10 Hz band, SDAC-TR-81-11, Teledyne Geotech, Alexandria, Virginia.

Duclaux, F., and L. Michaud, 1970. Conditions experimentales des tirs nucleaires souterrains francais au Sahara, 2961-1966, C. R. Acad. Sci Paris, 270B, 189-192.

Evernden, J. F., 1967. Magnitude determination at regional and near-regional distances in the US. Bull. Seism. Soc. Am., 57, p. 591-639.

Evernden, J. R. (1970), Magnitude versus yield of explosions, J. Geophys. Res., 75, p. 1028-1032.

Evernden, J. F., and D. M. Clark, 1970. Study of teleseismic P. II-Amplitude data, Phys. Earth planet. Int., 4, p. 24-31.

Ericsson, U., 1971a, Seismometric estimates of underground nuclear explosion yields. National Defense Research Institute, Stockholm, Report C 4464-26.

Ericsson, U., 1971b, A linear model for the yield dependence of magnitudes measured by a seismographic network. Geophys. J. Roy. Astron. Soc., 25, p. 49-69.

Fries, D. and T. Powell, 1964. Handbook: WWSSN, Univeristy of Michigan, Ann Arbor.

Gutenberg, B., and C. F. Richter (1956). Magnitude and energy of earthquakes, Ann. Geof. (Rome), 9, p. 1-15.

Hendrix, T., 1971. Guidebook 1, Geology G429 Field Geology in the Rocky Mountains, Indiana University, Bloomington, Indiana.

Holtedahl, O. and J. Dons, 1960. Geologisk Kart Over Norge, Oslo, Norway, 1:1,000,000.

Howe, W. and J. Koenig, 1961. The stratigraphic succession in Missouri, Geo. Surv. Wtr. Res., Rolla, Mo., p. 61.

Jones, F. B., L. T. Long, and J. H. McKee (1977). Study of attenuation and azimuthal dependence of seismic-wave propagation in the southeastern United States. Bull. Seism. Soc. Am. 67, p. 1503-1513.

King, P., 1969. Tectonic map of North America, U.S. Geological Survey, 1:5,000,000.

King, P. and H. Beikman, 1974. Geologic map of the United States, 1:2,500,000.

Lowry, W., 1971. Geological map of Blacksburg, Virginia area, Virginia Polytechnic Institute.

Marshall, P. D., D. L. Springer, and H. C. Rodean, 1979. Magnitude corrections for attenuation in the upper mantle, Geophys. J. Roy Astr. Soc., 57, p. 609-638.

Marshall, P. D., and P. W. Basham, 1972, Discrimination between earthquakes and underground explosions employing an improved M_s scale. Geophys. J. Roy. Astron Soc., 28, p. 431-458.

Noponen, J. and R. Cass, 1980. Survey of international seismic facilities and data management, AL-80-3, Teledyne Geotech, Alexandria, Virginia.

North, R. G., 1977, Station magnitude bias--its determination, causes, and effects, Massachusetts Institute of Technology, Lincoln Laboratory Technical Note 1977-24, Lexington, Massachusetts.

Nuttli, O. W., (1973). Seismic wave attenuation and magnitude relations for eastern North America, J. Geophys. Res., 78, p. 876-885.

Richter, C. F. (1958). Elementary Seismology, W. H. Freeman, San Francisco, 345-346.

Ringdal, F., (1976). Maximum likelihood estimation of seismic magnitude. Bull. Seism. Soc. Am., 66, p. 789-802.

Schmee, J., and G. H. Hahn (1979). A simple method for regression analysis with censored data. Technometrics, 21, p. 417-432.

Shumway, R. H., and R. R. Blandford, 1977, On detecting and estimating multiple arrivals from underground nuclear explosions, SDAC-TR-77-8, Teledyne Geotech, Alexandria, Virginia.

Springer, D. L. and R. Kinnaman, 1971. Seismic source summary for US underground nuclear explosions 1961-1970. Bull. Seism. Soc. Am., 61, p. 1073-1098.

Springer, D. L., and W. H. Hannon (1973). Amplitude-yield scaling for underground nuclear explosions, Bull. Seism. Soc. Am., 63, p. 477-500.

Springer, D. L., and R. L. Kinnaman 1975, Seismic source summary for US underground nuclear explosions, Bull. Seism. Soc. Am., 65, p. 343-349.

Stauder, W., et al, 1981. Central Mississippi Valley earthquake bulletin, 1 January - 31 March 1981, St. Louis University, p. 31.

Steinhart, J. and R. Meyer, 1961. Explosion studies of continental structure, Carnegie Institute of Washington, D. C.

Swan, A. V. (1969). Computing maximum likelihood estimates for the parameters of the normal distribution with grouped and censored data, J. Roy Statist. Soc. C, 18, p. 65-69.

Sweetser, E. I., and R. R. Blandford, 1973, Seismic distance-amplitude relations for short period P, P_{diff}, PP, and compressional core phases for 90°, SDAC-TR-73-9, Teledyne Geotech, P. O. Box 334, Alexandria, VA.

Veith, K. F., and G. E. Clawson, 1972, Magnitude from short period P-wave data. Bull. Seism. Soc. Am., 62, p. 435-452.

von Seggern, D., and R. Blandford, 1972, Source time functions and spectra for underground nuclear explosions, Geophys. J. R. Astr. Soc., 31, p. 83-97.

von Seggern, D., 1973, Joint magnitude determination and analysis of variance for explosion magnitude estimates. Bull. Seism. Soc. Am. 63, p. 827-845.

von Seggern, D., 1977, Intersite magnitude yield bias exemplified by the underground explosions Milrow, Boxcar and Handley, SDAC-TR-77-4, Teledyne Geotech, Alexandria, Virginia.

von Seggern, D., and D. W. Rivers, (1978). Comments on the use of truncated distribution theory for improved magnitude estimation. Bull. Seism. Soc. Am., 68, 1543-1548.

von Seggern, D., and S. S. Alexander, (1982), Magnitude of source, path and receiver effects for L_g waves from Nevada Test Site explosions and eastern North America earthquakes. (Submitted to Bull. Seism. Soc. Am.)

Geological Map of Asia and the Far East, Second Edition, U. N. Economic Commission for Asia and the Far East (ECAFE), U. N. Publication, No. 69-30632.

Generalized Cross Section of LRSM Stations, 1966. Teledyne Geotech, Garland, Texas.

Geological Map of the Continents of the World, 1973, Ministry of Geology, Moscow, 1:15,000,000.

University of Michigan, 1964, Handbook: World-Wide Standard Seismograph Network. Institute of Science and Technology, Ann Arbor, Michigan.

APPENDIX I

Joint Maximum Likelihood Estimation of Seismic Magnitude and Distance-Amplitude Dependence In the Presence of Clipped and Missed Signals

LIST OF FIGURES

LIST OF TABLES

MATHEMATICAL ABSTRACT

Several problems involving estimating seismic magnitudes and distance-amplitude slopes are considered when there may be severe censoring introduced by clipped or missed signals. It is shown that these classical situations as well as the one treated by Ringdal (1976) are all special cases of a doubly censored regression model. Maximum likelihood estimators for parameters such as station corrections, magnitude, and distance-amplitude corrections can be easily calculated using a version of the recently developed (Dempster et al.,1978) EM algorithm. Magnitude estimators are compared for several different models and a simulation study under conditions representative of papers in the seismic literature indicates that biases of .2 and .4 in conventional magnitude and slope ($\log_{10}$ amplitude versus $\log_{10}$ distance) estimators are essentially eliminated by the maximum likelihood procedure.

INTRODUCTION

The problem of estimating seismic magnitudes using amplitudes read at a number of recording stations is frequently complicated by the fact that the data may be heavily censored. This arises either because of clipping where all amplitudes exceeding a given upper limit are lost, or because of a missed signal which does not exceed a given lower threshold. If one simply averages the amplitudes for those stations which detect, without regard for those stations not recording, serious biases may result in the estimated magnitude levels.

The problem of estimating the mean and variance by maximum likelihood in the presence of singly censored data has been considered in the statistical literature by Cohen (1959), Swan (1969), with the initial seismic application given by Ringdal (1976) who exhibited via simulations the bias in the conventional estimator and the reduction in bias achieved by the maximum likelihood estimator (see also von Seggern and Rivers (1978)). Since the problem in this form involves only the two parameters μ and σ^2, simply scanning the likelihood non-linear function for a maximum in a restricted range was used in Ringdal (1976).

While the procedure described above is acceptable for a limited number of parameters lying in a specified range, it cannot be used in multiparameter situations such as those in which station effects or distance-amplitude slopes are to be estimated simultaneously. (See, for example, Richter (1958), Nuttli (1973), Bollinger (1973), Jones (1977), and Blandford et al (1980)). Some early results along this line were, however, achieved by Christoffersson et al., (1975). A further generalization of interest would be the extension to doubly censored (clipped and missed) and completely missed observations. The large number of parameters appearing in these more detailed models make classical non-linear methods like scoring or Newton-Raphson of little use and we employ a version of the recently developed E-M (Expectation-Maximization) algorithm which was suggested by Dempster et al (1977) for problems of this genre.

The general amplitude-distance models that we will use here are special cases of that used by von Seggern (1973) who represents the observed amplitude at station i for event j as

$$A_{ij} = \alpha S_i E_j (r_{ij}/10)^{-\gamma} \qquad (1)$$

for $i = 1,\ldots, n_s$, $j=1,\ldots, n_e$, where S_i is the effect of the ith station, E_j is the effect of the jth event, and r_{ij} is the distance in degrees from the ith event to the jth station. The parameter γ gives the rate of decay in the amplitude as a function of distance and is a constant scale factor. It is convenient to linearize equation (1) by taking logarithms to get

$$\log A_{ij} = \log \alpha + \log S_i + \log E_j - \gamma (r_{ij}/10) \qquad (2)$$

which can be converted to

$$a_{ij} = \mu + S_i + e_j + \beta d_{ij} + \epsilon_{ij} \qquad (3)$$

where the obvious identifications are made and ϵ_{ij} denote independent zero-mean additive Gaussian errors with common variance σ^2. The parameters are restricted to sum to zero, i.e. $\sum_{i=j}^{n_s} S_i = 0$, $\sum_{j=1}^{n_e} e_j = 0$ with the magnitude of the jth event interpreted as the parameter

$$m_j = \mu + e_j$$

for $j = 1,\ldots,n_e$. This is a standard linear regression model of the form used in Appendix I-A. The E-M algorithm has been used for the general linear regression model with singly censored data in Aitkin (1981) and in Schmee and Hahn (1979); we extend the results to include the possibility of double censoring and missing observations in Appendix I-A.

Although we will analyze several more general versions of equation (3) in the following sections, it is interesting to note that the E-M algorithm applied to the original Ringdal (1976) model

$$a_{i1} = \mu_1 + \epsilon_{i1} \qquad (4)$$

for $i = 1,\ldots, n_s$ gives the (r+1)st iterate from equation (3) as

$$\mu_1^{r+1} = n_s^{-1} \sum_{i=1}^{n_s} w_{i1}^r = w_{\cdot 1}^r \tag{5}$$

where $w_{i1}^r = a_{i1}$ if the observation is present and

$$w_{i1}^r = \begin{cases} \mu_1^r - \sigma_r \dfrac{\phi(Z_{i1}^r)}{\phi(Z_{i1}^r)} & \text{if } a_{i1} \leq t_{i1} \\ \mu_1^r + \sigma_r \dfrac{\phi(Z_{i2}^r)}{\phi(-Z_{i2}^r)} & \text{if } a_{i1} > t_{i2} \end{cases} \tag{6}$$

where

$$Z_{ij}^r = \frac{t_{ij} - \mu_1^r}{\sigma_r} \tag{7}$$

The variance is updated using equation (A16). Equations (5)-(7) display the updated estimator as an average of observations when one has them and corrected values when one only has thresholds (t_{i1}) and clipping levels (t_{i2}).

The next two sections consider two versions of equation (3) which are important in practical applications. The first is the estimation of magnitude for a global deployment of stations, so that B in (3) can be regarded as a known parameter (the B-factor). The second application focuses on estimating B for a more regional amplitude-distance study (see Blandford et al. (1981)) without estimating the station effects.

Joint Determination of Magnitudes and Station Corrections

A global distribution of amplitudes can often be corrected for distance using a known value for B, so that equation (3) might be rewritten as

$$a_{ij} = \mu + s_i + e_j + e_{ij}, \tag{8}$$

where the magnitude parameter of interest is

$$m_j = \mu + e_j \tag{9}$$

Table I shows a typical set of amplitude for $n_e=4$ events which theoretically could have been observed by each of $n_s=112$ stations. The observations are assumed to be in the four categories described in the Appendix with "<" denoting a category 1 observation known only to be below the given value, ">" denoting a category 2 observation known to have exceeded the given clipping level and " " denoting a no show or category 3 observation.

Again the equations for the E-M algorithm take on a simple form with

$$s_i^{r+1} = w_{i\cdot}^{\ r} - w_{\cdot\cdot}^{\ r} \tag{10}$$

$$m_j^{r+1} = w_{\cdot\ j}^{\ r} \tag{11}$$

estimating the station effect and magnitude value respectively. In this case, the "." notation signifies that a mean is to be taken over the appropriate subscript. The values of $w_{ij}^{\ r}$ are determined by (A13) and (A8), where in this case

$$\mu_{ij}^{\ r} = s_i^{\ r} + m_j^{\ r} \tag{12}$$

is the estimated mean at the rth iterate. One can take as initial values the station and event means.

Table II compares maximum likelihood estimators computed under three separate assumptions, with the original simple means of the event amplitudes in Table I. The means, shown in the first column, are quite high because each missed signal puts a threshold value into the average. All distances $0^\circ < \Delta < 180^\circ$ are used for estimation, and all signal measurements, even those <2 mm, are treated as signals and not as noise.

TABLE I

Observed P-Wave Amplitudes for Four Events

EVENT STA	SHOAL	PILEDRIVER	RUBIS	SAPHIR
AAE	< 5.44	< 5.72	5.29	5.81
AAM	5.10	5.66	5.29	----
ADE	< 5.99	< 5.96	< 5.58	< 5.88
AFI	< 5.41	< 5.59	< 5.96	< 6.14
AKU	----	5.27	----	6.08
ALQ	----	5.05	5.86	5.97
ANP	----	< 6.50	< 7.02	< 7.01
ANT	< 4.71	5.86	5.44	5.75
AQU	< 4.98	----	> 5.10	5.89
ARE	5.22	6.09	5.45	5.73
ATL	5.12	5.62	6.08	----
ATU	< 6.08	< 6.13	5.51	> 5.58
BAG	< 6.14	< 6.03	< 6.11	< 6.10
BEC	< 4.93	< 5.10	----	----
BHP	< 4.64	< 5.23	6.01	6.01
BKS	4.99	5.74	< 5.79	< 6.09
BLA	5.08	5.50	----	5.92
BOG	< 4.99	5.27	< 5.14	----
BOZ	4.81	5.36	5.82	6.07
BUL	----	5.67	5.44	5.58
CAR	5.69	5.85	5.08	5.32
CHG	----	----	----	5.68
COL	----	5.80	----	4.66
COP	< 5.13	< 5.61	5.44	< 5.56
COR	> 5.44	> 5.79	< 6.21	----
CTA	< 5.94	< 6.11	5.62	5.74
DAL	----	----	5.55	5.79
DAV	----	< 6.99	----	< 6.47
DUG	4.80	5.34	5.48	5.74
ESK	----	5.28	----	5.87
FLO	4.98	----	----	6.00
GDH	< 4.94	< 5.24	6.01	6.14
GEO	< 5.44	5.40	6.08	5.69
GIE	----	5.57	----	----
GOL	4.90	5.56	5.06	5.15
GSC	5.31	> 4.46	5.40	5.70
GUA	< 5.56	----	< 6.39	< 6.39
HKC	< 6.42	< 6.60	< 6.18	----
HLW	----	----	----	> 6.13
HNR	< 5.34	< 5.87	< 5.78	< 5.78
HOW	----	< 7.17	----	----
IST	< 5.72	< 5.96	----	----
JCT	----	5.53	----	----
JER	----	< 5.87	----	6.26
KEV	< 5.08	5.39	5.68	6.26
KIP	5.47	6.10	< 6.27	6.09
KOD	----	< 5.63	----	5.39

TABLE 1 (Continued)

KON	4.92	5.78	5.38	5.98
KTG	4.88	5.83	<4.96	5.22
LAH	<7.41	<7.25	----	<5.64
LEM	----	<5.43	----	----
LON	4.87	5.57	<5.12	5.63
LOR	----	5.70	----	----
LPA	----	<6.56	<6.09	<6.27
LPB	5.24	----	5.22	5.47
LPS	----	5.41	5.22	----
LUB	<5.03	----	----	6.45
MAT	----	>5.43	----	----
MAL	<4.91	5.35	6.25	6.65
MAN	<6.20	<6.72	<7.98	<6.88
MDS	5.07	----	5.38	5.55
MNN	4.42	----	5.40	5.73
MSH	----	<6.89	----	----
MUN	<5.61	<5.90	----	5.66
NAT	----	5.84	----	----
NAI	<5.31	5.95	5.43	>5.86
NDI	<5.74	<5.60	5.29	5.64
NNA	4.45	5.64	5.41	5.86
NOR	----	5.05	----	5.23
NUR	<4.83	5.48	5.12	5.42
OGD	5.08	5.10	----	5.66
OXF	----	5.98	----	----
PDA	<5.86	<5.38	----	<5.93
PMG	<5.70	<5.97	<5.41	5.54
POO	----	<5.26	----	5.64
PRE	----	----	5.30	5.43
PTO	----	5.31	5.32	5.69
PEL	----	5.47	----	6.04
QUE	<5.16	<5.88	4.70	4.93
QUI	<5.71	<6.00	<5.93	<6.23
RAB	5.57	----	<5.83	<6.19
RAR	----	<5.40	----	----
RCD	5.40	----	6.73	6.45
RIV	<6.68	<6.46	<5.30	<5.30
SBA	<4.92	5.27	5.50	<5.80
SDB	----	5.47	----	5.78
SCP	4.80	4.97	5.53	5.76
SEO	4.83	5.53	----	----
SHA	<5.15	5.64	5.86	6.16
SHI	<5.72	<5.63	5.81	>5.37
SHK	----	5.50	----	----
SHL	<5.39	<5.52	5.33	5.45
SJG	----	5.86	----	5.83
SNA	----	6.06	----	----
SNG	----	<5.55	----	----
SOM	----	<6.55	----	<6.92
SPA	5.11	5.99	5.45	5.82
STU	<4.86	5.47	5.90	6.18
TAB	----	<6.49	----	----
TAU	<5.77	<6.05	<5.25	<5.42
TOL	----	5.55	----	----

TABLE I (Continued)

TRI	<4.92	5.38	5.49	5.69
TRN	4.72	5.48	5.23	5.69
TUC	4.56	>5.32	5.89	----
UME	<4.50	5.76	5.27	5.60
VAL	<5.09	5.09	5.56	5.62
WEL	<6.67	<6.66	<6.29	<6.29
WES	4.52	4.95	5.45	5.63
WIN	4.93	5.90	5.01	5.50
HN-ME	----	----	----	----
NP-NT	----	----	----	----
CMC	----	4.99	----	5.54

TABLE II

Comparison of Event Means and Several Maximum Likelihood Estimators using Data of TABLE I

	(1)	(2)	(3)	(4)
SHOAL	5.24	4.81	4.84	4.81
PILEDRIVER	5.75	5.52	5.50	5.51
RUBIS	5.64	5.46	5.47	5.49
SAPHIR	5.86	5.75	5.74	5.77
σ			.38	.25

(1) Estimators computed as event means including censored observations.

(2) Maximum likelihood estimators for single event at a time using Ringdal (1976).

(3) Maximum likelihood estimators jointly for magnitudes excluding station corrections.

(4) Joint maximum likelihood estimators for magnitudes with station corrections.

The other columns are roughly comparable even though incorporating station corrections into the computations reduced σ (from .38 to .25), and the likelihood ratio test that the station effects are 0 gave

$$\chi^2 = -2\ (-149.82 + 40.17)$$
$$= 219.3$$

using (A17), where one may compare with a chi-square random variable with 112 degrees of freedom. Using the fact that for large degrees of freedom N the distribution is approximatley normal with mean N and variance 2N, we obtain Z = 7 which is highly significant.

The iterations leading to the maximum likelihood estimators in the last two columns take very little time with the 100 iterations required in the last case requiring less than two minutes on the IBM-360/44.

Estimation of the Distance-Amplitude Slope

For certain kinds of regional data (see Blandford et al. (1981), Nuttli (1973), Bollinger (1973), Jones et al. (1977)). The emphasis shifts to estimating a distance correction B in (3) where one may not have enough data to separate out a station effect. That is, we consider the model

$$a_{ij} = m_j + \beta d_{ij} + e_{ij} \tag{13}$$

for $j=1,\ldots, n_e$, $i=1,\ldots, n_i$ where $m_1, m_2,\ldots, m_{ne}$, β and σ^2 all need to be estimated, but we are primarily interested in the effects of missed and clipped signals on the value of β. Again, the E-M algorithm gives a simple updating procedure of the form

$$\beta_{r+1} = \frac{\sum_{ij} (d_{ij} - d_{\cdot j})\ (w_{ij}^r - w_{\cdot j}^r)}{\sum_{ij} (d_{ij} - d_{\cdot j})^2} \tag{14}$$

$$m_j^{r+1} = w_{\cdot j}^{\ r} - \beta_{r+1} d_{\cdot j}$$

with w_{ij}^{r} defined again by (A13) and (A8) where

$$\mu_{ij}^{r} = m_j^{r} + \beta_r d_{ij} \tag{15}$$

Note that unless σ is fixed, it is updated using (A16) at the end of each iteration. The initial estimator in each case was taken to be the least squares estimated using only the observed data since this is what corresponds to the usual approach in the seismological literature.

In order to evaluate the possible improvement due to using the maximum likelihood estimators, consider the linear model specified in (13) with eight stations recording five events at distance ranges of 1,3,5,7,9,13,17, and 21 degrees respectively. Suppose furthermore, that the upper and lower threshold are 104 m_μ (t_{2j}=4) and 102 m_μ (t_{1j}=2) respectively, and that amplitude decays as one over distance squared (β= -2). These values are a rough model of the data seen in Nuttli (1973).

Table III shows a collection of simulated amplitudes for five events where the magnitudes m_j,i=1,...,5 were drawn randomly from a standard magnitude frequency law which assumes that magnitudes ($\log_{10}$) are uniformly distributed over some arbitrary interval (2 to 5 for this example). (A constant of 2 is inserted in equations 14 so that both magnitude and threshold are realistic). The noise terms e_{ij} in equation (3) were taken as uncorrelated zero-mean normal variables with noise variance equal to .3, a typical value for the standard deviation of station magnitudes. The theoretical slope, as mentioned above, was β=-2. A further restriction was that at least three stations must detect in order to simulate the fact that an event is not used unless detected and located. The effect of the missing observations can be noticed in Figure 1 as a pronounced tendency to flatten out (decrease) the negative slope of the regression relation between amplitude and distance.

The estimators for the magnitude and slope parameters are shown in Table IV where the ordinary least squares solution ignores the clipped

TABLE III

Observed Amplitudes at Eight Stations for Five Events
Observed at a Theoretical Distance-Amplitude Slope of -2.00

Station	Events 1	2	3	4	5	Distance
1	5.41	**	5.69	**	5.88	-1.00
2	4.89	5.04	4.31	5.02	4.80	-.52
3	4.52	4.79	4.70	5.46	4.65	-.30
4	*	4.79	4.63	5.55	4.72	-.15
5	*	*	4.75	5.22	*	-.05
6	*	4.01	*	4.63	4.03	.11
7	*	*	*	4.24	*	.23
8	*	*	*	4.50	4.01	.32

* Censored below, i.e. failed to exceed the lower threshold (4)

** Clipped, i.e. exceeded upper threshold (6)

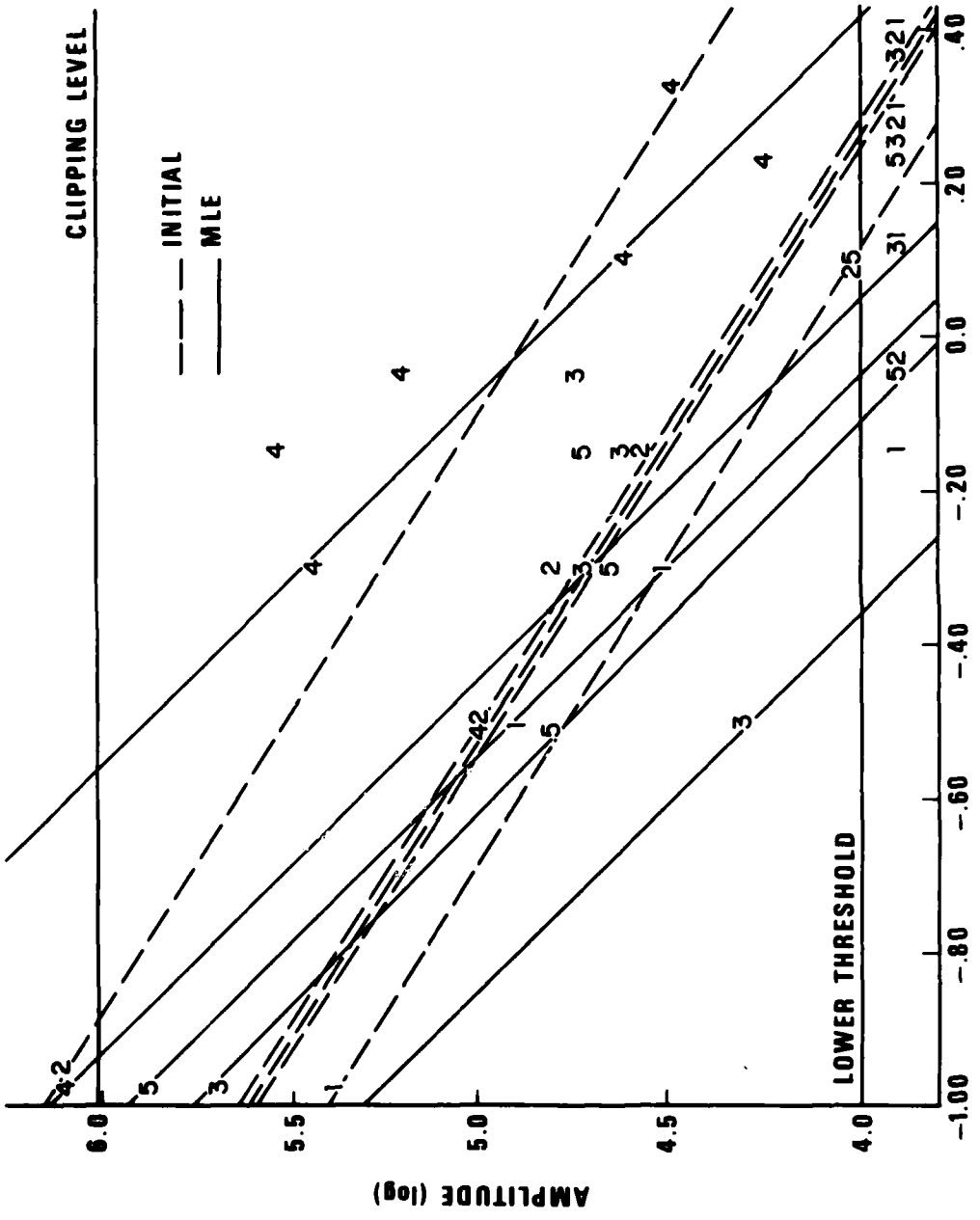

Figure 1 Illustration of effects of clipping and missing observations to reduce estimated amplitude-distance slope.

and censored amplitudes. The bias in the estimator for the slope is seen to be substantial; the value is -1.26 in this case as compared to the maximum likelihood procedure which yields a value of -2.04.

TABLE IV

Theoretical and Estimated Parameters

		Theoretical	Least Squares	Maximum Likelihood
Magnitudes	m_1	3.54	4.18	3.26
	m_2	4.20	4.34	4.09
	m_3	4.16	4.31	3.73
	m_4	4.88	4.88	4.84
	m_5	4.13	4.36	3.90
Slope	β	-2.00	-1.26	-2.04

In order to determine whether the bias observed in the above particular case was atypical, an experiment consisting of drawing a random set of amplitudes and performing seven iterations of the EM algorithm was repeated 40 times. The bias terms in Table V below were calculated by averaging the observed differences between the true and estimated values.

TABLE V

Average Bias of Least Squares (LSE) and Maximum Likelihood (MLE) Estimators in Simulation

	LSE	MLE
Magnitude	$-.20 \pm .02$*	$.05 \pm .02$
Slope	$-.37 \pm .07$	$-.02 \pm .08$

* ± 2 standard errors

These results indicate that the average magnitude and slope biases for the LSE are significantly greater than zero whereas the MLE slope bias is essentially zero and the magnitude bias is small. The results for the slope indicate that the average of the LSE's should be between -1.70 and -1.56 with 95% confidence whereas a 95% confidence interval for the

average slope produced by an MLE would be -2.08 to -1.90. The difference in slope is typical of that seen as differences between the authors mentioned in the Introduction for work in the same region. While we do not assert that any particular authors work is in error due to the particular technique used, we believe that use of the MLE techniques will enable differences due to geophysics to be more clearly detected.

We may also compare the mean square errors for the two procedures to determine whether or not the decrease in bias necessarily implies an increase in uncertainty. Table VI below gives the average mean square errors obtained by averaging the squared deviations between the theoretical and estimated values over the 40 replications.

TABLE VI

Average Mean Square Error for LSE and MLE in Simulation

	LSE	MLE
Magnitude	.087	.059
Slope	.194	.081

Although it can be seen that the MLE's have smaller values, the reductions are almost entirely due to the bias reduction. For example, since

$$\text{Variance} = \text{Mean Square Error} + (\text{Bias})^2,$$

we note that the average variance of the LSE of the slope parameter is .055 as compared to the variance of the MLE slope which is .081. Thus, it appears that the variances of the two estimators in this small sample case are roughly comparable.

The small scale simulation given above indicates that a rather substantial bias may exist for conventional estimators under conditions which are not unreasonable in the context of magnitude estimation. Although a broad range of experimental conditions have not been simulated, it seems reasonable to infer that the slope bias would

continue to be present whenever there are substantial numbers of clipped or missed signals. The simulation also indicates that the MLE tend to reduce the bias in the slope estimator by using the missing value information to steepen the negative slope, producing on the average, an estimator with a value closer to that indicated by results from events which are recorded without excessive clipping or censoring.

APPENDIX I-A

MAXIMUM LIKELIHOOD ESTIMATION FOR DOUBLY CENSORED REGRESSION MODELS

First of all, assume that there are four categories of observational data which may be available in any given situation so that the standard regression model may be written in the form

$$y_{ij} = \underline{x}'_{ij}\,\underline{\beta} + e_{ij},\ i = 0,1,2,3,\ j=1,\ldots,n_i \tag{A1}$$

for the jth observation in category i where $\underline{\beta}$ is a qx1 regression vector, with the qx1 design vector $\underline{x}_{ij}$ chosen to generate the appropriate linear combinations of the parameters $\beta_1, \beta_2, \ldots, \beta_q$. The subscript i denotes the censoring category of an observation according to the following classifications:

1. i=o denotes an observation where x_{oj} and y_{oj} are both available.
2. i=1 denotes that x_{1j} is observed but y_{1j} is known only to be below the threshold t_{1j}.
3. i=2 denotes that x_{2j} is observed but y_{2j} is known only to have exceeded the clipping threshold t_{2j}.
4. i=3 denotes that x_{3j} is observed but y_{3j} is not observed.

for notational ease, it will be convenient to define

$$\mu_{ij} = \underline{x}'_{ij}\,\underline{\beta} \tag{A2}$$

and note that if the errors e_{ij} are zero-mean independent standard normal variables with common variance σ_2, the likelihood functions can be written, using the fact the y_{ij} is normally distributed with mean μ_{ij} and variance σ^2. This means that the likelihood of the incomplete data sampler $y_o = (y_{o_1},\ldots,y_{o,n_o})$, $\underline{t}_1 = (t_{11},\ldots,t_{,n_1})'$, $\underline{t}_2 = (t_{21},\ldots,t_{2,n2})$ can be written as

$$\ell n\ L(\underline{y}_o,\underline{t}_1,\underline{t}_2|\underline{\beta},\sigma^2) = -\frac{n_o}{2}\,\ell n(2\pi\sigma^2) - \frac{1}{2\sigma^2}\sum_{j=1}^{n_o}(y_{oj}-\mu_{oj})^2 \tag{A3}$$

$$+ \sum_{j=1}^{n_1} \ell n\ \Phi(Z_{1j}) + \sum_{j=1}^{n_2} \ell n\ \Phi(-Z_{2j})$$

$$z_{ij} = \frac{t_{ij} - u_{ij}}{\sigma}, \quad i = 1,2; j = 1, \ldots n_i \tag{A4}$$

and

$$\Phi(u) = \int_{-\infty}^{u} \exp\{-\tfrac{1}{2} x^2\} \frac{dx}{\sqrt{2\pi}} \tag{A5}$$

The likelihood function could be treated in this form by differentiating (A3) twice with respect to β and σ^2 and applying an iterative Newton-Raphson or scoring algorithm to estimate the parameters. If there are a substantial number of parameters, this quickly becomes computationally intractable, as the corrections at each stage involve inversion of the 1/2(q+1) (q+2) dimensional information matrices.

A more manageable alternative procedure can be developed by employing the EM (Expectation-Maximization) algorithm as described in Dempster et al. This involves successive maximizations of the expectation of the complete data likelihood conditioned on the observed data. For example, if the complete data y_0, y_1, y_2, y_3, were available in the present case with $y_{ij} = (y_{i1}, y_{i2}, \ldots, y_{i,ni})$ for i = 0,1,2,3, the complete data likelihood would be written as

$$\ell n\ L\ (\underline{y}_0, \underline{y}_1, \underline{y}_2, \underline{y}_3 \mid \underline{\beta},\ \sigma^2) =$$
$$-\tfrac{1}{2} N \ln(2\pi\sigma^2) \left(-\frac{1}{2\sigma^2}\right) \sum_{i=o}^{3} \sum_{j=1}^{ni} (y_{ij} - \mu_{ij})^2 \tag{A6}$$

where u_{ij} is defined in equation (A2) and $N = \sum_{i=o}^{3} n_i$. If the current estimators for $\underline{\beta}$ and σ^2 are $\underline{\beta}_r$ and σ^2, the EM algorithm defines $\underline{\beta}_{r+1}$ and σ^2_{r+1} as the values of $\underline{\beta}$ and σ^2 maximizing the function

$$Q(\underline{\beta}, \sigma^2) = E_r \{\ell n\ L(\underline{y}_0, \underline{y}_1, \underline{y}_2, \underline{y}_3 \mid \beta, \sigma^2) \mid \underline{y}_0, \underline{y}_1, \langle \underline{t}_1, \underline{y}_2 \rangle \underline{t}_2\} \tag{A7}$$

where E_r denotes the expectation with respect to the parameter guesses at the current stage.

Now, by expanding $(y_{ij} - u_{ij})^2$, we note that all the terms in the conditional expectation given in (A6) can be determined when we know

$$E_r\,(y_{1j} | y_{1j} \leq t_{1j}) = \mu^r_{1j} - \sigma_r \frac{\phi(Z^r_{1j})}{\Phi(Z^r_{1j})} \tag{A8}$$

and $$E_r\,(y_{2j} | y_{2j} > t_{2j}) = \mu^r_{2j} + \sigma_r \frac{\phi(Z^r_{2j})}{\Phi(Z^r_{2j})}$$

$$E_r\,(y^2_{1j} | y_{1j} \leq t_{1j}) = \mu^{r\,2}_{1j} + \sigma^2_r - \sigma_r \frac{\phi(Z^r_{1j})}{\Phi(Z^r_{1j})}\,(t_{1j}+\mu^r_{1j}) \tag{A9}$$

$$E_r\,(y_{2j}{}^2 | y_{2j} > t_{2j}) = \mu^{r\,2}_{2j} + \sigma^2_r + \sigma_r \frac{\phi(Z^r_{2j})}{\Phi(Z^r_{2j})}\,(t_{2j}+\mu^r_{2j})$$

where μ^r_{ij} and Z^r_{ij} are equations (A2) and (A4) with $\underset{\sim}{\beta}_r$ and $\sigma_r{}^2$ replacing $\underset{\sim}{\beta}$ and σ^2. The function $\phi(\cdot)$ is defined as the standard normal density

$$\phi(u) = (2\pi)^{-\frac{1}{2}} \exp\{-\tfrac{1}{2} u^2\}. \tag{A10}$$

Then, returning to (A6) and (A7), we note that the succeeding estimators can be determined by maximizing

$$\begin{aligned} Q(\beta,\sigma^2) = {} & -\tfrac{1}{2}N\ell n(2\pi\sigma^2) - \frac{1}{2\sigma^2}\sum_{j=1}^{n_0}(y_{0j}-\mu_{0j})^2 \\ & -\frac{1}{2\sigma^2}\sum_{j=1}^{n_1} E_r\{(y_{1j}-\mu_{1j})^2 | y_{1j} \leq t_{1j}\} \\ & -\frac{1}{2\sigma^2}\sum_{j=1}^{n_2} E_r\{(y_{2j}-\mu_{2j})^2 | y_{2j} > t_{2j}\} \\ & -\frac{1}{2\sigma^2}\sum_{j=1}^{n_3} E_r\{(y_{3j}-\mu_{3j})^2\} \end{aligned} \tag{A11}$$

with respect to $\underline{\beta}$ and σ^2.

Now in order to maximize the above expression, note that it may be written in the form

$$Q(\underline{\beta},\sigma^2) = \frac{1}{2} N \ln (2\pi\sigma^2)$$

$$-\frac{1}{2\sigma^2}\left[\sum_{ij} v_{ij}^r - 2\underline{\beta}' \sum_{ij} \underline{x}_{ij} w_{ij}^r + \underline{\beta}' \sum_{ij} \underline{x}_{ij}\underline{x}_{ij}\underline{\beta}\right] \qquad \text{(A12)}$$

where

$$w_{ij}^r = \begin{cases} y_{ij}, & i=0 \\ E_r(y_{ij} \mid y_{ij} \leq t_{ij}), & i=1 \\ E_r(y_{ij} \mid y_{ij} > t_{ij}), & i=2 \\ (\mu_{ij}^r), & i=3 \end{cases} \qquad \text{(A13)}$$

and

$$v_{ij}^r = \begin{cases} y_{ij}^2, & i=0 \\ E_r(y_{ij}^2 \mid y_{ij} \leq t_{ij}), & i=1 \\ E_r(y_{ij}^2 \mid y_{ij} > t_{ij}), & i=2 \\ (\mu_{ij}^r)^2+\sigma_r^2, & i=3 \end{cases} \qquad \text{(A14)}$$

with the conditional expectations given in (A8) and (A9). Some algebra shows that $Q(\underline{\beta},\sigma^2)$ is maximized for

$$\underline{\beta}_{r+1} = \left(\sum_{ij} \underline{x}_i \underline{x}_{ij}'\right)^{-1} \sum_{ij} \underline{x}_{ij} w_{ij}^r \qquad \text{(A15)}$$

and

$$\sigma_{r+1}^2 = N^{-1}\left[\sum_{j=1}^{n_0}(y_{0j}-\mu_{0j}^r)^2+\sigma_r^2\left(N-n_0+\sum_{j=1}^{n_2}\frac{\phi(Z_{2j}^r)}{\Phi(Z_{2j}^r)}Z_{2j}^r - \sum_{j=1}^{n_1}\frac{\phi(Z_{1j}^r)}{\Phi(Z_{1j}^r)}Z_{1j}^r\right)\right] \qquad \text{(A16)}$$

It is convenient to notice that (A15) is just the ordinary least squares or maximum likelihood solution evaluated at the observations w^r_{ij} as defined in (A13). This facilitates the application of the technique to the special cases described in the text.

The basic iterative procedure can be started with initial estimators for β and σ^2 derived from maximum likelihood estimators derived by fixing the censored values at the upper or lower thresholds. Then, equations (A15) and (A16) can be applied to generate successive iterates for β_r and σ_r^2 until the incomplete data log likelihood given by (A3) is maximized.

It should be noted that, for reasonably large samples certain hypotheses can be tested by comparing the log likelihoods computed under the various models. For example, if H_Ω estimates n_Ω parameters and H_ω is a restriction of H_Ω which estimates n_ω parameters then

$$\chi^2 = -2(\ln L_\omega - \ln L_\Omega) \qquad \text{(A-17)}$$

is distributed as chi-square random variable with $(n_\Omega - n_\omega)$ degrees of freedom if H_ω is true.

APPENDIX II

CRUSTAL MODELS

Crustal Models

Station	Model T	α	β	ρ	Quality	Geology	Reference
AAE	1.0	5.5	3.2	2.6	Good	1000 m. Tertiary basalts	U. of Mich.(1964)
	1.2	4.5	2.5	2.5		on 1200 m. Mesozoic sandstone	
	∞	6.1	3.6	2.7		and limestone on basement	
AAM	0.1	1.8	0.5	2.0	Good	glacial drift	U. of Mich.(1964)
	0.1	2.5	1.3	2.2		shale	
	1.6	6.0	3.5	2.5		limestone, dolomite	
	∞	6.1	3.6	2.7		granite	
ADE	1.0	6.1	3.6	2.7	Fair	PreCambrian deposits	U. of Mich.(1964)
	∞	6.1	3.6	2.7			
AFI	1.0	6.1	3.6	2.7	Poor	Pleistocene basalt	U. of Mich(1964)
	∞	6.1	3.6	2.7			
AKU	1.0	6.1	3.6	2.7	Poor	basalt	Noponen and Cass(1980)
	∞	6.1	3.6	2.7			
ALQ	1.0	6.1	3.6	2.7	Good	PreCambrian granite	U. of Mich.(1964)
	∞	6.1	3.6	2.7			
ANP	1.0	5.9	3.4	2.7	Poor	Pleistocene andesite	U. of Mich.(1964)
	∞	6.1	3.6	2.7		lava flows	
ANT	1.0	5.5	3.2	2.6	Poor	limestone	U. of Mich.(1964)
	∞	6.1	3.6	2.7			
AQU	2.0	5.5	3.2	2.6	Poor	limestone over	U. of Mich.(1964)
	∞	6.1	3.6	2.7		granite	
ARE	0.8	5.7	3.3	2.7	Good	80 m. unweathered volcanics	U. of Mich.(1964)
	∞	6.1	3.6	2.7		over basement	
ATL	1.0	6.1	3.6	2.7	Good	PreCambrian migmatites	King and Beikman(1974)
	∞	6.1	3.6	2.7			
ATU	1.0	5.0	2.8	2.5	Poor	Mesozoic rocks?	Choubert and Faure-Muret(1980)
	∞	6.1	3.6	2.7			
BAG	1.0	5.6	3.2	2.6	Poor	limestone	U. of Mich.(1964)
	∞	6.1	3.6	2.7			
BEC	1.0	2.0	1.0	2.0	Poor	aeolian limestone	U. of Mich.(1964)
	∞	6.1	3.6	2.7			
BHP	0.8	3.0	1.6	2.3	Poor	(no info., used nearby	Steinhart and Meyer(1961)
	3.4	5.0	2.9	2.5		model)	
	∞	6.1	3.6	2.7			
BKS	10.0	5.5	3.2	2.6	Good	velocity model	Steinhart and Meyer(1961)
	∞	6.5	3.8	2.7			
BLA	0.8	6.0	3.5	2.5	Good	dolomite	Lowry(1971)
	1.6	3.0	1.6	2.4		shale	
	0.6	6.0	3.5	2.6		dolomite	
	∞	6.1	3.6	2.7		PreCambrian sediments	
BOG	1.0	4.5	2.5	2.6	Poor	sandstone	U. of Mich.(1964)
	∞	6.1	3.6	2.7			
BOZ	2.8	3.6	2.0	2.5	Good	velocity model	Steinhart and Meyer(1961)
	∞	6.1	3.6	2.7			
BUL	1.3	5.4	3.1	2.6	Poor	lava, used nearby	Steinhart and Meyer(1961),
	∞	6.2	3.6	2.7		model	U. of Mich.(1964)
CAR	1.0	4.5	2.5	2.5	Poor	Cretaceous schists	U. of Mich.(1964)
	∞	6.1	3.6	2.7		granite	
CHG	1.0	6.1	3.6	2.7	Fair	granite	U. of Mich.(1964)
	∞	6.1	3.6	2.7			
CMC	1.0	6.1	3.6	2.7	Good	PreCambrian sediments	King(1969)
	∞	6.1	3.6	2.7		and volcanics	
COL	1.0	6.1	3.6	2.7	Good	PreCambrian metamorphics	King(1969)
	∞	6.1	3.6	2.7			
COP	1.0	5.4	3.1	2.6	Poor	Tertiary (limestone?)	U. of Mich.(1964)
	∞	6.1	3.6	2.7			

Crustal Models

Station	Model T	Model α	Model β	Model ρ	Quality	Geology	Reference
COR	2.2	4.4	2.5	2.3	Good	weathered basalt, velocity model	Berg et al(1966), U. of Mich.(1964)
	7.7	5.5	3.2	2.5			
	∞	6.6	3.9	2.7			
CTA	1.0	6.1	3.6	2.7	Fair	granodiorite	U. of Michigan(1964)
	∞	6.1	3.6	2.7			
DAL	1.3	5.5	3.2	2.6	Good	4150' Cretaceous sediments on Paleozoic	U. of Mich.(1964)
	∞	6.1	3.6	2.7			
DAV	1.0	6.4	3.2	2.8	Good	Paleozoic basalt	Choubert and Faure-Muret(1980)
	∞	6.4	3.2	2.8			
DUG	1.0	6.1	3.6	2.7	Fair	granite	U. of Mich.(1964)
	∞	6.1	3.6	2.7			
ESK	1.0	5.0	2.8	2.6	Poor	Permian continental facies	Choubert and Faure-Muret(1980)
	∞	6.1	3.6	2.7			
FLO	0.1	5.0	2.8	2.6	Good	clay on Mississippian limestone, velocity model	Howe and Koenig(1961), Stauder et al(1981), U. of Mich.(1964)
	2.0	5.6	3.3	2.65			
	∞	6.2	3.6	2.7			
GDH	1.0	6.1	3.6	2.7	Fair	gneiss	U. of Mich.(1964)
	∞	6.1	3.6	2.7			
GEO	1.0	6.1	3.6	2.7	Good	PreCambrian diorite	U. of Mich.(1964)
	∞	6.1	3.6	2.7			
GIE	1.0	6.4	3.2	2.8	Poor	extrusives	Choubert and Faure-Muret(1980)
	∞	6.4	3.2	2.7			
GOL	1.0	6.1	3.6	2.7	Good	PreCambrian granite and pegmatite	U. of Mich.(1964)
	∞	6.1	3.6	2.7			
GSC	1.0	6.1	3.6	2.7	Fair	granite	U. of Mich.(1964)
	1.0	6.1	3.6	2.7			
GUA	0.2	3.7	2.0	1.9	Poor	volcanic tuff	Noponen and Cass(1980)
	∞	6.1	3.6	2.7			
HKC	1.0	6.1	3.6	2.7	Poor	granite and diorite	ECAFE(1971)
	∞	6.1	3.6	2.7			
HLW	1.0	4.0	2.2	2.6	Poor	Cretacous limestone	U. of Mich.(1964)
	∞	6.1	3.6	2.7			
HN-ME	10.0	5.9	3.4	2.7	Good	dolomite and slate granite	Teledyne Geotech(1966)
	∞	6.4	3.6	2.7			
HNR	1.0	4.5	2.5	2.5	Poor	sandstone on Miocene limestone	U. of Mich.(1964)
	∞	6.1	3.6	2.7			
HOW	0.2	2.0	1.0	2.0	Poor	alluvium	Noponen and Cass(1980)
	∞	6.1	3.6	2.7			
IST	1.0	6.1	3.6	2.7	Fair	Devonian graywacke	U. of Mich.(1964)
	∞	6.1	3.6	2.7			
JCT	1.0	4.0	2.2	2.6	Poor	lower Cretaceous	King and Beikman(1974)
	∞	6.1	3.6	2.7			
JER	1.0	3.6	2.0	2.4	Poor	Upper Cretaceous	Choubert and Faure-Muret(1980)
	∞	6.1	3.6	2.7			
KEV	1.0	6.1	3.6	2.7	Fair	granulite	U. of Mich.(1964)
	∞	6.1	3.6	2.7			
KIP	1.0	6.1	3.6	2.7	Fair	Tertiary basalt	U. of Mich.(1964)
	∞	6.1	3.6	2.7			
KOD	0.2	2.0	1.0	2.0	Poor	alluvium	Noponen and Cass(1980)
	∞	6.1	3.6	2.7			
KON	1.0	6.1	3.6	2.7	Fair	granite	Holtedahl and Dons(1960)
	∞	6.1	3.6	2.7			
KTG	1.0	6.1	3.6	2.7	Fair	gneiss	Noponen and Cass(1980)
	∞	6.1	3.6	2.7			

Crustal Models

Station	Model T	Model α	Model β	Model ρ	Quality	Geology	Reference
LAH	0.3	2.0	1.0	2.0	Fair	1200' alluvium, bedrock is probably schist	U. of Mich.(1964)
	∞	6.1	3.6	2.7			
LEM	1.0	6.4	3.2	2.8	Poor	volcanics?	ECAFE(1971)
	∞	6.4	3.2	2.8			
LON	1.0	6.1	3.6	2.7	Good	volcanics on granodiorite batholith	U. of Mich.(1964)
	∞	6.1	3.6	2.7			
LOR	1.0	4.5	2.5	2.5	Poor	Middle Jurassic?	Choubert and Faure-Muret(1980)
	∞	6.1	3.6	2.7			
LPA	0.2	2.0	1.0	2.0	Poor	600' Quaternary loess	U. of Mich.(1964)
	∞	6.1	3.6	2.7			
LPB	1.0	3.6	2.0	2.5	Poor	clay and sand	U. of Mich.(1964)
	∞	6.1	3.6	2.7			
LPS	1.0	6.1	3.6	2.7	Fair	granite	U. of Mich.(1964)
	∞	6.1	3.6	2.7			
LUB	1.0	3.6	2.0	2.4	Poor	Pliocene continental deposits	King and Beikman(1974)
	∞	6.1	3.6	2.7			
MAL	1.0	5.5	3.2	2.6	Poor	Tertiary limestone	U. of Mich.(1964)
	∞	6.1	3.6	2.7			
MAN	1.0	6.1	3.6	2.7	Fair	Tertiary tuff over meta-volcanics and basement	U. of Mich.(1964)
	∞	6.1	3.6	2.7			
MAT	1.0	6.4	3.2	2.8	Poor	Quaternary extrusives?	Choubert and Faure-Muret(1980)
	∞	6.4	3.2	2.8			
MDS	1.0	6.1	3.6	2.7	Poor	quartzite	U. of Mich.(1964)
	∞	6.1	3.6	2.7			
MNN	1.3	5.6	3.2	2.6	Good	130' sandstone on 2000' dolomite on granite	U. of Mich.(1964)
	∞	6.1	3.6	2.7			
MSH	1.0	6.1	3.6	2.7	Good	PreCambrian gneiss and schist	ECAFE(1971)
	∞	6.1	3.6	2.7			
MUN	1.0	6.1	3.6	2.7	Fair	granite	U. of Mich.(1964)
	∞	6.1	3.6	2.7			
NAI	1.0	6.1	3.6	2.7	Good	lavas and pyroclastics on basement gneiss	Noponen and Cass(1980)
	∞	6.1	3.6	2.7			
NAT	1.0	3.6	2.0	2.4	Poor	Paleocene and Neocene	Ministry of Geology(1973)
	∞	6.1	3.6	2.7			
NDI	1.0	4.3	2.4	2.5	Poor	quartzite and sandstone	Noponen and Cass(1980)
	∞	6.1	3.6	2.7			
NNA	1.0	6.1	3.6	2.7	Fair	gabbro	Noponen and Cass
	∞	6.1	3.6	2.7			
NOR	1.0	4.5	2.5	2.5	Poor	Pennsylvanian to Cretaceous	King(1969)
	∞	6.1	3.6	2.7			
NUR	1.0	6.1	3.6	2.7	Good	PreCambrian gneiss	U. of Mich.(1964)
	∞	6.1	3.6	2.7			
OXF	1.0	3.6	2.0	2.4	Poor	Eocene	King and Beikman(1974)
	∞	6.1	3.6	2.7			
PDA	1.0	4.7	2.7	2.6	Fair	ash and scoria	U. of Mich.(1964)
	∞	6.1	3.6	2.7			
PEL	1.0	4.5	2.5	2.6	Poor	Cretaceous	Ministry of Geology(1973)
	∞	6.1	3.6	2.7			
PMG	0.5	2.0	1.0	2.0	Poor	Eocene and Oligocene tuff and agglomerate	U. of Mich.(1964)
	∞	6.1	3.6	2.7			
PRE	1.0	6.1	3.6	2.7	Good	PreCambrian sediments	U. of Mich.(1964)
	∞	6.1	3.6	2.7			
POO	1.0	6.1	3.6	2.7	Poor	lava flows	Noponen and Cass(1980)
	∞	6.1	3.6	2.7			

Crustal Models

Station	Model T	Model α	Model β	Model ρ	Quality	Geology	Reference
PTO	1.0	6.1	3.6	2.7	Fair	Paleozoic granite	Choubert and Faure-Muret(1980)
	∞	6.1	3.6	2.7			
QUE	1.0	4.5	2.5	2.5	Poor	Cretaceous limestone and shale	U. of Mich.(1964)
	∞	6.1	3.6	2.7			
QUI	0.1	4.5	2.5	2.6	Poor	75 m. hard clay and sand on bedrock	U. of Mich.(1964)
	∞	6.1	3.6	2.7			
RAB	1.0	6.1	3.6	2.7	Fair	basalt	U. of Mich.(1964)
	∞	6.1	3.6	2.7			
RAR	1.0	6.4	3.2	2.8	Fair	basalt	Noponen and Cass(1980)
	∞	6.4	3.2	2.8			
RCD	0.6	2.5	1.3	2.3	Good	sandstone and shale	Hendrix(1971)
	0.1	3.0	1.6	2.4		sandstone	
	0.1	6.0	3.0	2.5		limestone and dolomite	
	0.1	2.5	1.3	2.2		shale	
	∞	6.1	3.6	2.7		basement	
RIV	0.3	4.5	2.5	2.5	Good	280 m. Triassic sandstone over	U. of Mich.(1964)
	0.6	5.0	2.9	2.5		600 m. Triassic sandstone and	
	1.5	5.5	3.2	2.6		shale on 1500 m. Permian or	
	∞	6.1	3.6	2.7		Carboniferous sediments	
RK-ON	1.0	6.1	3.6	2.7	Good	PreCambrian granites and gneisses	King(1969)
	∞	6.1	3.6	2.7			
SBA	1.0	6.1	3.6	2.7	Poor	volcanics	U. of Mich.(1964)
	∞	6.1	3.6	2.7			
SCP	1.0	6.1	3.6	2.7	Fair	Ordovician limestone	U. of Mich.(1964)
	∞	6.1	3.6	2.7			
SDB	1.0	6.1	3.6	2.7	Good	PreCambrian granite	Choubert and Faure-Muret(1980)
	∞	6.1	3.6	2.7			
SEO	1.0	6.1	3.6	2.7	Good	PreCambrian granite	Choubert and Faure-Muret(1980)
	∞	6.1	3.6	2.7			
SHA	0.5	2.5	1.3	2.0	Poor	Pliocene clay on Miocene estuary deposits	U. of Mich.(1964)
	∞	6.1	3.6	2.7			
SHI	1.0	4.2	2.4	2.5	Poor	hard Eocene limestone	Noponen and Cass(1980)
	∞	6.1	3.6	2.7			
SHK	1.0	6.1	3.6	2.7	Fair	granite	Noponen and Cass(1980)
	∞	6.1	3.6	2.7			
SHL	1.0	5.0	2.8	2.6	Poor	limestone and sandstone	Noponen and Cass(1980)
	∞	6.1	3.6	2.7			
SJG	1.0	6.4	3.2	2.8	Poor	Mesozoic extrusives	Choubert and Faure-Muret(1980)
	∞	6.4	3.2	2.8			
SNA	0.5	3.5	1.9	1.0	Poor	ice	Noponen and Cass(1980)
	∞	6.1	3.6	2.7			
SNG	1.0	6.1	3.6	2.7	Poor	granite?	ECAFE(1971)
	∞	6.1	3.6	2.7			
SOM	1.0	3.6	2.0	2.4	Poor	Quaternary deposits	Ministry of Geology(1973)
	∞	6.1	3.6	2.7			
SPA	2.7	3.5	2.0	2.0	Poor	2700 m. ice	U. of Mich.(1964)
	∞	6.1	3.6	2.7			
STU	1.0	5.0	2.8	2.5	Poor	lower Jurassic	Choubert and Faure-Muret(1980)
	∞	6.1	3.6	2.7			
TAB	1.0	6.4	3.2	2.8	Poor	Tertiary extrusive?	Choubert and Faure-Muret(1980)
	∞	6.4	3.2	2.8			
TAU	0.2	2.0	1.0	2.5	Fair	Tertiary lacustrine sands	U. of Mich.(1964)
	0.2	5.9	3.2	2.6		and clays on Jurassic intrusives	
	0.2	5.8	3.4	2.6		Permian siltstones and limestones	
	1.0	5.9	3.4	2.7		pre-Permian	
	∞	6.1	3.6	2.7			

Crustal Models

Station	Model T	Model α	Model β	Model ρ	Quality	Geology	Reference
TOL	0.2 0.8 ∞	2.0 4.0 6.1	1.0 2.2 3.6	2.0 2.5 2.7	Poor	alluvium on Miocene rock	U. of Mich.(1964)
TRI	1.0 ∞	3.6 6.1	2.0 3.6	2.4 2.7	Poor	Paleocene to Eocene	Choubert and Faure-Muret(1980)
TRN	1.0 ∞	6.1 6.1	3.6 3.6	2.7 2.7	Poor	decomposed phyllite	U. of Mich.(1964)
TUC	4.3 ∞	4.8 6.1	2.8 3.6	2.1 2.7	Poor	metamorphic bedrock	U. of Mich.(1964)
UME	1.0 ∞	6.1 6.1	3.6 3.6	2.7 2.7	Fair	gneiss and pegmatite	U. of Mich.(1964)
VAL	1.0 ∞	6.1 6.1	3.6 3.6	2.7 2.7	Fair	Devonian continental facies	Choubert and Faure-Muret(1980)
WEL	1.0 ∞	4.0 6.1	2.2 3.6	2.6 2.7	Poor	Mesozoic graywacke	U. of Mich.(1964)
WES	1.0 ∞	6.1 6.1	3.6 3.6	2.7 2.7	Good	Paleozoic metavolcanics	U. of Mich.(1964)
WIN	2.0 ∞	6.1 6.1	3.6 3.6	2.7 2.7	Fair	2000 m. schist	U. of Mich.(1964)